Office of Naval Research
Contract N00014-87-K-0117

Technical Report No. 9

A CONTINUUM MODEL FOR PHASE TRANSFORMATION IN THERMOELASTIC SOLIDS

by

Qing Jiang*

Division of Engineering and Applied Science
California Institute of Technology
Pasadena, California

July, 1989

* Present address: Department of Civil Engineering, University of Manitoba, Winnipeg, Manitoba, Canada R3T 2N2

ABSTRACT

Under suitable programs of mechanical or thermal loading, many solid materials are capable of undergoing phase transformations from one crystal structure to another. The austenite-martensite transformation that occurs in a variety of metallic alloys, including the so-called shape-memory materials, provides an example. The present paper represents an effort to model coupled thermo-mechanical effects in the macroscopic response of solids that arise from the occurrence of phase transformations. A Helmholtz free energy potential is constructed to describe the thermo-mechanical response of the hypothetical material to be considered here. As a function of shear strain, the potential is non-convex in a certain range of temperature; this feature is essential for the modeling of phase transformations. Apart from some general preliminary considerations pertaining to finite thermoelasticity, the analysis is carried out in the context of a simple problem, idealized from an experiment, in which an annular cylinder is deformed to a state of radically symmetric, finite anti-plane shear in the presence of differing inner and outer surface temperatures. After constructing all radially symmetric weak solutions involving at most a single surface of discontinuity of strain or temperature gradient, we determine the implications for quasi-static motions of the second law of thermodynamics. The thermo-mechanical phase transformation-induced hysteresis, residual deformation and stress relaxation effects exhibited by this model are discussed. The results concerning creep rate as predicted by the present model are in qualitative agreement with the laboratory observations. Finally, the shape-memory effect as predicted by the present thermo-mechanical model in the setting of finite anti-plane shear has been simulated numerically; a number of pictures selected from the simulation are included.

TABLE OF CONTENTS

1. Introduction

Many solid materials are capable of undergoing phase transformations from one crystal structure to another under suitable programs of mechanical or thermal loading. The austenite-martensite transformation that occurs in a variety of metallic alloys, including the so-called shape-memory materials, provides a well known example. Experimental observations of the behavior of such materials are discussed, for example, in [1]. The development of models for the macroscopic thermo-mechanical response of such materials represents an active, current area of study in the continuum mechanics of solids. Examples of such investigations may be found in [2]-[10].

The problem of modeling the macroscopic response of a solid undergoing a phase transformation is an inherently nonlinear one. Most of the studies reported in [2]-[10] were carried out within the framework of the purely mechanical theory of finite elastostatics; they are, therefore, appropriate only for the modeling of load-induced phase transformations taking place at a given temperature. In these studies, the interface between two material phases emerges as a surface of strain discontinuity in the relevant equilibrium field. Not all elastic potentials - or strain energy functions - are capable of sustaining equilibrium fields exhibiting such singular surfaces. Those that do have this capability correspond to what have been called non-elliptic elastic materials, because they lead to displacement equations of equilibrium that, although elliptic for infinitesimal deformations, lose their ellipticity for a certain range of finite strain.

When surfaces of strain discontinuity occur in equilibrium elastic fields, quasi-static motions - regarded as one-parameter families of equilibrium states - become dissipative. Dissipation occurs in the sense that the rate of work of the external forces acting on a portion of the body no longer coincides with the rate of increase of stored energy. Their difference may be represented as an integral over the slowly moving surface bearing the strain discontinuity of a fictitious "driving traction" -

or "Eshelby force" [11] - multiplied by the velocity of the moving singular surface. In this isothermal, purely mechanical setting, the disparity between the rate of external work and the rate of storage of energy may thus be regarded as arising because work must be done to move the phase boundary.

Equilibrium boundary value problems in the theory of non-elliptic elastic materials suffer a massive breakdown in the uniqueness of solution. Quasi-static motions in such materials may visit any of the infinitely many available equilibrium states consistent with the boundary conditions. In order to render the macroscopic response of such materials determinate, it is necessary to supplement the constitutive description of the material by a relation that specifies the "kinetics" of the phase transformation, or the rate at which particles transform from one phase to another. The incorporation of such a kinetic relation into the theory has been shown to predict isothermal macroscopic response that is in qualitative agreement with experiments, at least in the one-dimensional theory of tension experiments [13,1].

The present paper represents an effort to model coupled thermo-mechanical effects on the macroscopic response of solids that arise from the occurrence of phase transformations. Apart from some general preliminary considerations pertaining to finite thermoelasticity in Chapter 2, our analysis is carried out in the context of finite anti-plane shear, which is the simplest setting in which to study finite deformations. Chapter 3 is devoted to the construction of a Helmholtz free energy potential intended to describe the thermo-mechanical response of the hypothetical material to be considered here. This material is designed to model phase transitions in somewhat the same sense as the van der Waals model describes the gas-liquid transition. As a function of strain, the potential is non-convex in a certain range of temperature.

Motivated by the possibility of large strains arising from phase transformations in the earth's mantle, Sammis and Dein [14] carried out a simple laboratory

experiment designed to show that creep could indeed be generated by the occurrence of a phase transformation induced by both thermal and mechanical loads. Their experiment, which is described in detail in Chapter 4, is one that lends itself to modeling by finite anti-plane shear, and Chapters 4 through 8 are devoted to the formulation and analysis of such a model. In particular, the implications for quasi-static motions of the second law of thermodynamics are determined in Chapter 5, and construction of a model kinetic relation is undertaken in Chapter 6. Chapter 7 deals with the phase transformation-induced hysteresis, residual deformation and stress relaxation effects exhibited by the model. The results presented in Chapter 8 concerning creep rate as predicted by the present model of the Sammis-Dein experiment are in qualitative agreement with the laboratory observation reported in [14].

Chapter 9 illustrates the shape-memory effect as predicted by the present simple thermo-mechanical model in the setting of finite anti-plane shear.

2. Preliminaries on continuum mechanics

2.1 Global and local versions of balance laws

Consider a body B that, in a reference configuration, occupies a region R in three-dimensional Euclidean space. A motion of the body on a time interval $L \equiv [t_0, t_1]$ is characterized by a one-parameter family of invertible mappings $\hat{\mathbf{y}}(\cdot, t) : R \longmapsto R_t$, with

$$\mathbf{y} = \hat{\mathbf{y}}(\mathbf{x}, t) = \mathbf{x} + \mathbf{u}(\mathbf{x}, t) \quad for \quad (\mathbf{x}, t) \in R \times L. \tag{2.1}$$

We assume that the deformation $\hat{\mathbf{y}}$, or equivalently the displacement $\mathbf{u}$, is continuous with piecewise continuous first and second derivatives on $R \times$L. Let $\mathbf{F}(\mathbf{x}, t) = Grad\, \hat{\mathbf{y}}(\mathbf{x}, t)$ stand for the deformation gradient tensor, and assume that for each $t \in L$, and $\mathbf{x} \in R$, the Jaccobian determinant of mapping (2.1) is positive:

$$J(\mathbf{x}, t) = det\, \mathbf{F}(\mathbf{x}, t) > 0. \tag{2.2}$$

Let $\rho(\mathbf{x})$ denote the mass density of B at the point $\mathbf{x}$ in the reference region R, $\mathbf{b}(\mathbf{x}, t)$ the body force per unit mass, and $\boldsymbol{\sigma}$(x,t) the nominal stress tensor during the motion. At each t, we require $\rho(\cdot)$ and $\mathbf{b}(\cdot, t)$ to be continuous on R, while $\boldsymbol{\sigma}(\cdot, t)$ is to be piecewise continuous with a piecewise continuous gradient on R. Let $\rho^*(\mathbf{y}, t)$ be the mass density of B at the point $\mathbf{y}$ in the region R_t occupied by the body at the instant t, and we require $\rho^*(\cdot, t)$ to be piecewise continuous for each t. For each $t \in L$, the balance laws for mass, linear and angular momentum require

$$\int_{D_t} \rho^* dv = \int_D \rho dv; \tag{2.3}$$

$$\int_{\partial D} \boldsymbol{\sigma} \mathbf{n} da + \int_D \rho \mathbf{b} dv = \frac{d}{dt} \int_D \rho \dot{\mathbf{u}} dv; \tag{2.4}$$

$$\int_{\partial D} \hat{\mathbf{y}} \wedge \boldsymbol{\sigma}\mathbf{n}da + \int_D \hat{\mathbf{y}} \wedge \rho\mathbf{b}dv = \frac{d}{dt}\int_D \hat{\mathbf{y}} \wedge \rho\dot{\mathbf{u}}dv; \tag{2.5}$$

respectively, for all regular subregions $D \subset R$. The superposed dot denotes the partial derivative with respect to t at fixed $\mathbf{x}$.

Next, let $\mathbf{q}(\mathbf{x}, t)$ denote the nominal heat flux vector, $\xi(\mathbf{x}, t)$ the heat supply per unit mass and $\epsilon(\mathbf{x}, t)$ the internal energy per unit mass. At each t, we suppose that $\xi(\cdot, t)$ is continuous on R and that $\mathbf{q}(\cdot, t)$ is piecewise continuous with a piecewise continuous gradient on R. The internal energy $\epsilon(\cdot, \cdot)$ is required to be piecewise continuous with piecewise continuous first derivatives on $R \times L$. The first law of thermodynamics requires that at each instant t,

$$\begin{aligned}\int_{\partial D} \boldsymbol{\sigma}\mathbf{n} \cdot \dot{\mathbf{u}}da + \int_D \rho\mathbf{b} \cdot \dot{\mathbf{u}}dv + \int_{\partial D} \mathbf{q} \cdot \mathbf{n}da + \int_D \rho\xi dv \\ = \frac{d}{dt}\int_D \rho(\epsilon + \dot{\mathbf{u}} \cdot \dot{\mathbf{u}}/2)dv,\end{aligned} \tag{2.6}$$

for every regular subregion $D \subset R$. Finally, let $\theta(\mathbf{x}, t)$ denote the absolute temperature and $\eta(\mathbf{x}, t)$ the entropy per unit mass. At each t, we assume that $\theta(\cdot, t)$ is continuous with a piecewise continuous gradient on R, while $\eta(\cdot, \cdot)$ is assumed to be piecewise continuous with piecewise continuous first derivatives on $R \times L$. The rate of entropy production in a region D in R is defined by

$$\Gamma(t; D) = \frac{d}{dt}\int_D \rho\eta dv - \int_{\partial D} \mathbf{q} \cdot \mathbf{n}/\theta da - \int_D \rho\xi/\theta dv. \tag{2.7}$$

The Clausius-Duhem version of the second law of thermodynamics requires

$$\Gamma(t; D) \geq 0 \quad D \subset R, \ t \in L. \tag{2.8}$$

At a fixed instant t, localization of the balance laws (2.3) - (2.6) and the inequality (2.8) at a point $\mathbf{x}$ at which all fields are smooth yields the following:

$$\begin{gathered}\rho^* J = \rho, \\ Div\,\boldsymbol{\sigma} + \rho\mathbf{b} = \rho\ddot{\mathbf{u}}, \\ \boldsymbol{\sigma}\mathbf{F}^T = \mathbf{F}\boldsymbol{\sigma}^T, \\ \boldsymbol{\sigma}\cdot\dot{\mathbf{F}} + Div\,\mathbf{q} + \rho\xi = \rho\dot{\epsilon}, \\ Div\,(\mathbf{q}/\theta) + \rho\xi/\theta \leq \rho\dot{\eta}.\end{gathered} \tag{2.9}$$

On the other hand, suppose that S(t) is a regular surface in R at time t across which some or all of the thermo-mechanical quantities suffer jump discontinuities. Localization of (2.3) - (2.8) at a point $\mathbf{x}$ on S(t) yields the following jump conditions:

$$\begin{gathered}[\![\rho^* J]\!] = 0, \\ [\![\boldsymbol{\sigma}\mathbf{n}]\!] + \rho[\![\dot{\mathbf{u}}]\!]V_n = 0, \\ [\![\boldsymbol{\sigma}\mathbf{n}\cdot\dot{\mathbf{u}}]\!] + [\![\rho(\epsilon + \frac{1}{2}\dot{\mathbf{u}}\cdot\dot{\mathbf{u}})]\!]V_n + [\![\mathbf{q}\cdot\mathbf{n}]\!] = 0, \\ [\![\rho\eta]\!]V_n + [\![\mathbf{q}\cdot\mathbf{n}/\theta]\!] \leq 0,\end{gathered} \tag{2.10}$$

where

$$V_n = \mathbf{V}\cdot\mathbf{n}, \tag{2.11}$$

and $\mathbf{V} = \mathbf{V}(\mathbf{x}, t)$ is the velocity of the moving surface S(t) at the point $\mathbf{x}$. The unit normal $\mathbf{n}$ on the singular surface S(t) is chosen such that $V_n \geq 0$; if $V_n > 0$, the positive side of S(t) is the side into which $\mathbf{V}$ (and therefore $\mathbf{n}$) points. If g(x,t) denotes a generic field quantity that jumps across S(t), we write $[\![g(\mathbf{x}, t)]\!] = g^+(\mathbf{x}, t) - g^-(\mathbf{x}, t)$, where $g^+(\mathbf{x}, t)$ and $g^-(\mathbf{x}, t)$ stand for the limiting values of g at the point $\mathbf{x}$ on S(t) from the positive and negative sides, respectively.

Conversely, the field equations (2.9) together with the jump conditions (2.10) imply the global balance laws (2.3) - (2.6) and (2.8).

In addition to the jump conditions listed in (2.10), one can derive the following kinematic results through the smoothness requirements imposed on the deformation (2.1):

$$[\mathbf{F}]\mathbf{m} = \mathbf{0}, \quad [\dot{\mathbf{u}}] = -[\mathbf{F}]\mathbf{V} \quad on \quad S(t), \tag{2.12}$$

where **m** is any vector tangent to the singular surface S(t).

2.2 Rate of entropy production

With help of the field equations (2.9) and the jump conditions (2.10) and (2.12), Abeyaratne and Knowles [12] derived the following alternate representation for the rate of entropy production defined in (2.7):

$$\Gamma(t; D) = \Gamma_{loc}(t; D) + \Gamma_{con}(t; D) + \Gamma_s(t; D), \tag{2.13}$$

where

$$\Gamma_{loc}(t; D) = \int_D (\rho\dot{\eta}\theta + \boldsymbol{\sigma}\cdot\dot{\mathbf{F}} - \rho\dot{\epsilon})/\theta \, dv, \tag{2.14}$$

$$\Gamma_{con}(t; D) = \int_D \mathbf{q}\cdot Grad\,\theta/\theta^2 \, dv, \tag{2.15}$$

$$\Gamma_s(t; D) = \int_{S(t)\cap D} [\rho\psi - \frac{1}{2}(\boldsymbol{\sigma}^+ + \boldsymbol{\sigma}^-)\cdot\mathbf{F}]V_n/\theta \, da, \tag{2.16}$$

while ψ is the Helmholtz free energy per unit mass, defined by

$$\psi(\mathbf{x}, t) = \epsilon(\mathbf{x}, t) - \theta(\mathbf{x}, t)\eta(\mathbf{x}, t) \quad on\ R \times L. \tag{2.17}$$

In (2.13), the total rate of entropy production $\Gamma(t; D)$ at the instant t in the subregion $D \subset R$ is decomposed into three parts: Γ_{loc} arises from local dissipation in the material away from the singular surface; Γ_{con} is the entropy production rate due to heat conduction; finally, Γ_s represents the entropy production rate due to the moving singular surface S(t). No constitutive assumptions are made in the derivation of (2.13) - (2.16).

The driving traction $f(\mathbf{x}, t)$ acting on the surface of discontinuity S(t) is defined by

$$f(\mathbf{x},t) = \rho(\mathbf{x})[\![\psi(\mathbf{x},t)]\!] - \frac{1}{2}(\boldsymbol{\sigma}^{+}(\mathbf{x},t) + \boldsymbol{\sigma}^{-}(\mathbf{x},t)) \cdot [\![\mathbf{F}(\mathbf{x},t)]\!], \quad for \quad \mathbf{x} \in S(t),\ t \in L. \tag{2.18}$$

Then, from (2.16) and (2.18), $\Gamma_s(t;D)$ can be written as

$$\Gamma_s(t;D) = \int_{S(t)\cap D} f V_n/\theta \, da, \tag{2.19}$$

and localization of (2.8) at point $\mathbf{x}$ on S(t) yields

$$f(\mathbf{x},t)V_n(\mathbf{x},t) \geq 0 \quad for \quad \mathbf{x} \in S(t),\ t \in L. \tag{2.20}$$

2.3 Finite thermoelasticity

We now specify that the body at hand is thermoelastic and assume that there are a free energy potential $\hat{\Psi}$ and a heat-flux-response function $\hat{\mathbf{q}}$ such that, for every thermodynamic process,

$$\psi = \hat{\Psi}(\mathbf{F},\theta), \tag{2.21}$$

$$\mathbf{q} = \hat{\mathbf{q}}(\mathbf{F},\theta,Grad\,\theta), \tag{2.22}$$

$$\boldsymbol{\sigma} = \rho\hat{\Psi}_{\mathbf{F}}(\mathbf{F},\theta), \quad or \quad \sigma_{ij} = \rho\partial\hat{\Psi}(\mathbf{F},\theta)/\partial F_{ij}, \tag{2.23}$$

$$\eta = -\hat{\Psi}_{\theta}(\mathbf{F},\theta), \quad or \quad \eta = -\partial\hat{\Psi}(\mathbf{F},\theta)/\partial\theta. \tag{2.24}$$

Objectivity requires that

$$\hat{\Psi}(\mathbf{QF},\theta) = \hat{\Psi}(\mathbf{F},\theta), \quad \hat{\mathbf{q}}(\mathbf{QF},\theta,\mathbf{v}) = \hat{\mathbf{q}}(\mathbf{F},\theta,\mathbf{v}), \tag{2.25}$$

for every nonsingular tensor $\mathbf{F}$, every proper orthogonal tensor $\mathbf{Q}$, every positive scalar θ and every vector $\mathbf{v}$.

Because of (2.17), (2.21), (2.23) and (2.24), Γ_{loc} defined by (2.14) vanishes identically for thermoelastic materials, and hence localization of (2.8) away from the singular surface S(t) yields

$$\hat{r}(\cdot,\cdot,\cdot,\mathbf{v})\cdot\mathbf{v}\geq 0, \quad \textit{for any vector } \mathbf{v}. \tag{2.26}$$

This supplies a restriction on the heat-flux-response function $\hat{q}$.

2.4 Isotropic thermo-elastic materials

We assume from here on that the body is thermo-mechanically isotropic, so that

$$\hat{\Psi}(\mathbf{FQ},\theta)=\hat{\Psi}(\mathbf{F},\theta), \quad \hat{\mathbf{q}}(\mathbf{FQ},\theta,\mathbf{Q}^T\mathbf{v})=\mathbf{Q}^T\hat{\mathbf{q}}(\mathbf{F},\theta,\mathbf{v}), \tag{2.27}$$

for every nonsingular tensor $\mathbf{F}$, every proper orthogonal tensor $\mathbf{Q}$, every positive scalar θ and every vector $\mathbf{v}$. Here $\mathbf{Q}^T$ denotes the transpose of $\mathbf{Q}$. It follows that the free energy $\hat{\Psi}(\mathbf{F},\theta)$ depends on $\mathbf{F}$ only through the deformation invariants:

$$\hat{\Psi}(\mathbf{F},\theta)=\bar{\Psi}(I_1,I_2,I_3,\theta), \tag{2.28}$$

where the fundamental scalar invariants I_1, I_2, I_3 are defined by

$$\begin{aligned} &I_1(\mathbf{C})=tr\mathbf{C}, \quad I_2(\mathbf{C})=[(tr\mathbf{C})^2-tr(\mathbf{C^2})]/2,\\ &I_3(\mathbf{C})=det\mathbf{C}, \qquad \mathbf{C}=\mathbf{F}^T\mathbf{F}. \end{aligned} \tag{2.29}$$

In the presence of isotropy, (2.23) takes the form

$$\boldsymbol{\sigma}=2\rho\bar{\Psi}_{I_1}\mathbf{F}+2\rho\bar{\Psi}_{I_2}(I_1\mathbf{1}-\mathbf{FF}^T)\mathbf{F}+2I_3\rho\bar{\Psi}_{I_3}\mathbf{F}^{-T}, \tag{2.30}$$

where $\mathbf{1}$ stands for the identity tensor and $\mathbf{F}^{-T}$ is the transpose of the inverse of the nonsingular tensor $\mathbf{F}$.

We assume from now on that the heat-flux-response function $\hat{\mathbf{q}}$ depends on $Grad\,\theta$ linearly, i.e.,

$$\hat{\mathbf{q}}(\mathbf{F},\theta,\mathbf{v}) = \mathbf{K}(\mathbf{F},\theta)\mathbf{v}, \tag{2.31}$$

for every nonsingular tensor $\mathbf{F}$, positive scalar θ and vector $\mathbf{v}$. Here $\mathbf{K}$ is called the heat conductivity tensor and, in the presence of isotropy, $\mathbf{K}$ takes the form

$$\mathbf{K}(\mathbf{F},\theta) = \phi_0\mathbf{1} + \phi_1\mathbf{F}^{\mathrm{T}}\mathbf{F} + \phi_2(\mathbf{F}^{\mathrm{T}}\mathbf{F})^2, \tag{2.32}$$

where $\phi_k = \phi_k(I_1, I_2, I_3, \theta)$, k = 0, 1, 2.

By assuming that ϕ_1 and ϕ_2 both vanish identically, we obtain the generalized Fourier law:

$$\hat{\mathbf{q}}(\mathbf{F},\theta,Grad\,\theta) = \phi_0(I_1, I_2, I_3, \theta)Grad\,\theta. \tag{2.33}$$

ϕ_0 is required to be non-negative by (2.26).

2.5 Thermo-mechanical states of anti-plane shear

Suppose R is a cylindrical region and let $\mathbf{X} = (0; \mathbf{e_1}, \mathbf{e_2}, \mathbf{e_3})$ be a rectangular cartesian frame with the unit vector $\mathbf{e_3}$ parallel to the generators of the cylinder. Consider a time-independent thermo-mechanical state of anti-plane shear, in which

$$y_1 = x_1, \quad y_2 = x_2, \quad y_3 = x_3 + u(x_1, x_2), \quad \theta = \theta(x_1, x_2), \tag{2.34}$$

where the out-of-plane displacement u and the temperature θ are both defined on the cross-section D of R. In the given frame, the deformation gradient tensor $\mathbf{F}$ has components:

$$F_{\alpha\beta} = \delta_{\alpha\beta}, \quad F_{\alpha 3} = 0, \quad F_{3\alpha} = u_{,\alpha} \quad F_{33} = 1. \tag{2.35}$$

Here $\delta_{\alpha\beta}$ is the Kronecker delta, Latin and Greek subscripts have the respective ranges 1, 2, 3, and 1, 2, and repeated subscripts are summed over the appropriate

range. A subscript proceded by a comma indicates partial differentiation with respect to the corresponding x-coordinate. The fundamental invariants I_1, I_2, I_3 are given by

$$I_1 = I_2 = 3 + \gamma^2, \quad I_3 = 1, \tag{2.36}$$

where $\gamma \equiv |Grad\, u| = \sqrt{u_{,\alpha}\, u_{,\alpha}}$. When specialized to the anti-plane shear (2.34), the constitutive statement (2.30) yields the components of nominal stress σ as

$$\begin{aligned} \sigma_{\alpha\beta} &= [2\tilde{\Psi}_{I_1} + 2(2+\gamma^2)\tilde{\Psi}_{I_2} - p]\delta_{\alpha\beta} - 2\tilde{\Psi}_{I_2} u_{,\alpha}\, u_{,\beta}\,, \\ \sigma_{\alpha 3} &= [-2\tilde{\Psi}_{I_2} + p]u_{,\alpha}\,, \quad \sigma_{3\alpha} = 2[\tilde{\Psi}_{I_1} + \tilde{\Psi}_{I_2}]u_{,\alpha}\,, \\ \sigma_{33} &= 2\tilde{\Psi}_{I_1} + 4\tilde{\Psi}_{I_2} - p, \end{aligned} \tag{2.37}$$

where we have written

$$\tilde{\Psi} = \tilde{\Psi}(I_1, I_2, \theta) = \rho\bar{\Psi}(I_1, I_2, 1, \theta), \quad p = -2\rho\bar{\Psi}_{I_3}(I_1, I_2, 1, \theta), \tag{2.38}$$

and from (2.36),

$$I_1 = I_2 = 3 + \gamma^2. \tag{2.39}$$

In the absence of body forces, the momentum balance $(2.9)_2$ yields

$$[p - 2\tilde{\Psi}_{I_1} - 2(2+\gamma^2)\tilde{\Psi}_{I_2}]_{,\alpha} + [2\tilde{\Psi}_{I_2} u_{,\alpha}\, u_{,\beta}]_{,\beta} = 0, \quad \alpha = 1, 2, \tag{2.40}$$

and

$$[M(\gamma, \theta)u_{,\beta}]_{,\beta} = 0, \tag{2.41}$$

where the arguments I_1 and I_2 of p and $\tilde{\Psi}$ in (2.40) are given by (2.39), and M in (2.41) is defined by

$$M(\gamma,\theta) = 2[\tilde{\Psi}_{I_1}(I_1,I_2,\theta) + \tilde{\Psi}_{I_2}(I_1,I_2,\theta)]_{I_1=I_2=3+\gamma^2}. \tag{2.42}$$

In the absence of heat sources, the first law of thermodynamics $(2.9)_4$ takes the simple form

$$[k(\gamma,\theta)\theta_{,\alpha}]_{,\alpha} = 0, \tag{2.43}$$

where k is defined by

$$k(\gamma,\theta) = \phi_0(3+\gamma^2, 3+\gamma^2, 1, \theta). \tag{2.44}$$

In view of the fact that p, M and k are expressed in terms of u and θ through (2.38), (2.42) and (2.44), the equations (2.40), (2.41) and (2.43) actually comprise four differential equations for two unknowns u and θ, and hence constitute an over-determined system in general. Without some restriction on the material properties, one would expect that only very special solutions of (2.41) and (2.43) would also satisfy (2.40). We say that a thermoelastic material is capable of sustaining anti-plane shear if, for every domain D, every solution u, θ of (2.41) and (2.43) also satisfies (2.40). In general, an isotropic thermoelastic material need not be capable of sustaining anti-plane shear. We turn next to a sub-class of such materials which do sustain anti-plane shear.

3. A special class of thermo-elastic materials

As shown by Knowles [15], all homogeneous, isotropic incompressible hyperelastic materials whose elastic potential W depends only on the first fundamental scalar invariant I_1 are capable of sustaining anti-plane shear. Materials in this class have been called generalized Neo-Hookean materials by Gurtin [10] because the Neo-Hookean model of rubber elasticity is included among them. Generalized Neo-Hookean materials have proved to be useful in studying nonlinear effects – especially qualitative ones – in the simplest possible setting: that of finite anti-plane shear; see, for example, [10], [16], [17].

Generalized Neo-Hookean materials, being incompressible, do not permit the useful incorporation of thermal effects of the kind essential in the study of thermoelasticity. Jiang and Knowles [18] have introduced a class of homogeneous, isotropic, compressible hyperelastic materials that do not suffer from this limitation and at the same time are capable of sustaining finite anti-plane shear. The thermoelastic counterpart of the class of materials studied in [18] is characterized by the Helmholtz free energy per unit reference volume as follows:

$$\tilde{\Psi}(I_1, I_2, I_3, \theta) = \tilde{\Psi}(I_1, \theta) + \tilde{\Psi}_{I_1}(I_1, \theta)\tilde{g}(I_3, \theta) + g(I_3, \theta), \tag{3.1}$$

where θ is the absolute temperature, and $\tilde{\Psi}$, f and g are functions on $(0, \infty) \times (0, \infty)$, with $\tilde{\Psi}$ differentiable three times, $\tilde{g}$ and g twice. One can show that the necessary and sufficient condition for a material of type (3.1) to be capable of sustaining finite anti-plane shear is the following

$$\tilde{g}(1, \theta) = 0, \quad \tilde{g}_{I_3}(1, \theta) = -1, \quad g_{I_3}(1, \theta) = constant, \quad \forall\, \theta > 0. \tag{3.2}$$

In all the following discussion, we choose $g_{I_3}(1, \theta)$ to be zero, which implies that the undeformed state is unstressed. Without loss of generality, we set $g(1, \theta) = 0$

and thus $\tilde{\Psi}$ represents the Helmholtz free energy density associated with volume-preserved deformations*.

The components of nominal stress in (2.37) reduce to

$$\sigma_{\alpha\beta} = 0, \quad \sigma_{\alpha 3} = \sigma_{3\alpha} = M(\gamma,\theta)u_{,\alpha}, \quad \sigma_{33} = 0, \quad on\ D, \tag{3.3}$$

where M is given by (2.42). The true (or Cauchy) stress $\boldsymbol{\tau}$ is given in terms of $\boldsymbol{\sigma}$ and $\mathbf{F}$ by

$$\boldsymbol{\tau} = \boldsymbol{\sigma}\mathbf{F}^T/J. \tag{3.4}$$

From (3.4), (3.3) and (2.35), one can determine the true stresses τ_{ij}:

$$\tau_{\alpha\beta} = 0, \quad \tau_{\alpha 3} = \tau_{3\alpha} = M(\gamma,\theta)u_{,\alpha}, \quad \tau_{33} = \gamma^2 M(\gamma,\theta). \tag{3.5}$$

We introduce the shear stress response function $\hat{\tau}(\gamma,\theta)$ by

$$\hat{\tau}(\gamma,\theta) = \gamma M(\gamma,\theta), \quad for\ (\gamma,\theta) \in [0,\infty) \times (0,\infty), \tag{3.6}$$

then the magnitude of the resultant of shear stresses $\tau_{\alpha 3}\mathbf{e}_\alpha$ is then given by

$$\sqrt{\tau_{\alpha 3}\tau_{\alpha 3}} = \hat{\tau}(\gamma,\theta). \tag{3.7}$$

One can show that for θ fixed, the equilibrium equation in x_3-direction (2.41) is elliptic [15] for any out-of-plane displacement u if and only if

$$M(\gamma,\theta)\frac{\partial\hat{\tau}(\gamma,\theta)}{\partial\gamma} > 0 \qquad \forall\gamma \geq 0. \tag{3.8}$$

or equivalently,

$$\tilde{\Psi}_{I_1}(3+\gamma^2,\theta)[\tilde{\Psi}_{I_1}(3+\gamma^2,\theta) + 2\gamma^2\tilde{\Psi}_{I_1 I_1}(3+\gamma^2,\theta)] > 0, \quad \forall\,\gamma \geq 0. \tag{3.9}$$

* Note that, $\bar{\Psi}(I_1,I_2,I_3,\theta) = \tilde{\Psi}(I_1,\theta)$ if $I_3 = 1$, by (3.2).

Consider a deformation of a body composed of a homogeneous, isotropic thermoelastic material with the Helmholtz free energy potential $\bar{\Psi}(I_1, I_2, I_3, \theta)$. If λ_1, λ_2, λ_3, are the principal stretches of the deformation, one has

$$I_1 = \lambda_1^2 + \lambda_2^2 + \lambda_3^2, \quad I_2 = \lambda_1^2\lambda_2^2 + \lambda_2^2\lambda_3^2 + \lambda_3^2\lambda_1^2, \quad I_3 = \lambda_1^2\lambda_2^2\lambda_3^2. \tag{3.10}$$

Let

$$\hat{\Psi}(\lambda_1, \lambda_2, \lambda_3, \theta) = \bar{\Psi}(I_1, I_2, I_3, \theta), \tag{3.11}$$

where I_1, I_2 and I_3 are expressed in terms of the stretches λ_i by (3.10). It follows from (3.4), (2.30), (3.11) and (3.10) that the principal true stresses τ_1, τ_2 and τ_3 are given by

$$\tau_i = \frac{\lambda_i}{J}\frac{\partial \hat{\Psi}}{\partial \lambda_i}(\lambda_1, \lambda_2, \lambda_3, \theta), \quad (\textit{no sum on } i). \tag{3.12}$$

The Baker-Ericksen inequalities require that the greater of any two principal stresses shall correspond to the greater of the corresponding two principal stretches when the stretches are distinct; thus

$$(\tau_i - \tau_j)(\lambda_i - \lambda_j) > 0 \quad \textit{if } \lambda_i \neq \lambda_j, \quad i, j = 1, 2, 3. \tag{3.13}$$

For the material described by (3.1), one finds from (3.1), (3.10) - (3.12) that the Baker-Ericksen inequalities (3.13) hold [18] if and only if

$$\tilde{\Psi}_{I_1}(I_1, \theta) + \tilde{\Psi}_{I_1 I_1}(I_1, \theta) f(I_3, \theta) > 0, \quad \textit{for } 0 < I_3 < (I_1/3)^3. \tag{3.14}$$

When specialized to the anti-plane shear (2.34), (3.14) reduces to

$$\tilde{\Psi}_{I_1}(3 + \gamma^2, \theta) > 0, \quad \textit{for } \gamma > 0, \tag{3.15}$$

or equivalently

$$M(\gamma,\theta) > 0, \quad for\ \gamma > 0. \tag{3.16}$$

In deformations other than anti-plane shear, issues such as the form taken by the ellipticity conditions for the material characterized by (3.1) are more difficult to analyze. The implication of idealizations in (3.1) is thus not fully clear. One idealization that is apparent from (3.2) is the fact that the reference configuration is unstressed at any temperature.

We shall be concerned with a special case of the materials (3.1) whose Helmholtz free energy for volume-preserving deformations is given by

$$\tilde{\Psi}(I_1,\theta) = \frac{1}{12}\mu(\theta)(I_1-3)[I_1-3-4\beta(\theta)\sqrt{I_1-3}+6\alpha^2]+h(\theta), \tag{3.17}$$

$$for\ I_1 \geq 3,\ \theta > 0;$$

with

$$\beta(\theta) = \beta_0(\alpha/\beta_0)^{m^2(1-\theta/\theta_0)^2}, \quad for\ \theta > 0; \tag{3.18}$$

Here, the functions μ and h are defined and twice continuously differentiable on $(0,\infty)$ and are required to satisfy

$$\mu(\theta) > 0, \quad h''(\theta) < 0, \quad for\ \theta > 0; \tag{3.19}$$

where the constant θ_0 is a charateristic temperature and α, β_0, m are dimensionless positive constants subject to the restriction

$$(\beta_0/\alpha)^2 > 4/3, \tag{3.20}$$

this allows the material to achieve some unstressed but deformed states at certain range of temperature (see eq.(3.28) and Fig. 3a) and this feature is essential to model shape-memory behavior (see Chapter 9).

For convenience, let

$$\Psi(\gamma,\theta) = \tilde{\Psi}(3+\gamma^2,\theta), \quad for\ \gamma \geq 0,\ \theta > 0; \tag{3.21}$$

by (3.6), (2.42) and (3.17), the shear stress response function $\hat{\tau}$ at constant temperature of this material is given by

$$\hat{\tau}(\gamma,\theta) = \Psi_\gamma(\gamma,\theta) = \frac{1}{3}\mu(\theta)\gamma(\gamma^2 - 3\beta(\theta)\gamma + 3\alpha^2). \tag{3.22}$$

In this special case, the ellipticity condition (3.8) reduces to

$$(\gamma^2 - 3\beta(\theta)\gamma + 3\alpha^2)(\gamma^2 - 2\beta(\theta)\gamma + \alpha^2) > 0, \quad \forall\, \gamma \geq 0. \tag{3.23}$$

From (3.18), one can see that (3.23) fails for $\theta \in [\theta_*, \theta^*]$ where

$$\theta_* = (1 - \frac{1}{m})\theta_0, \quad \theta^* = (1 + \frac{1}{m})\theta_0. \tag{3.24}$$

Let A_1, A_2 and A_3 be the sets of points in the strain-temperature plane defined by

$$\begin{aligned} A_1 &= \{(\gamma,\theta)/\ \gamma \geq 0\ for\ \theta < \theta_*\ and\ 0 \leq \gamma < \gamma_M(\theta)\ for\ \theta \in [\theta_*, \theta^*]\}, \\ A_2 &= \{(\gamma,\theta)/\ \gamma_M(\theta) < \gamma < \gamma_m(\theta)\ for\ \theta \in (\theta_*, \theta^*)\}, \\ A_3 &= \{(\gamma,\theta)/\ \gamma \geq 0\ for\ \theta > \theta^*\ and\ \gamma > \gamma_m(\theta)\ for\ \theta \in [\theta_*, \theta^*]\}, \end{aligned} \tag{3.25}$$

where the functions of temperature $\gamma_M(\theta)$ and $\gamma_m(\theta)$ are defined on $[\theta_*, \theta^*]$ by

$$\gamma_m(\theta) = \beta(\theta) + \sqrt{\beta^2(\theta) - \alpha^2}, \quad \gamma_M(\theta) = \beta(\theta) - \sqrt{\beta^2(\theta) - \alpha^2}. \tag{3.26}$$

By (3.21) and (3.17),

$$\Psi_{\gamma\gamma}(\gamma,\theta) = \mu(\theta)(\gamma^2 - 2\beta(\theta)\gamma + \alpha^2) \begin{cases} < 0 & \text{on } A_2; \\ = 0 & \text{on } \partial A_2; \\ > 0 & \text{on } A_1 \cup A_3. \end{cases} \tag{3.27}$$

Here, $\Psi(\cdot,\theta)$ is convex for $\theta \in (0,\theta_*] \cup [\theta^*,\infty)$ and non-convex for $\theta \in (\theta_*,\theta^*)$. Correspondingly, the shear stress response function $\hat{\tau}(\cdot,\theta)$ is monotonic for $\theta \in (0,\theta_*] \cup [\theta^*,\infty)$ and non-monotonic for $\theta \in (\theta_*,\theta^*)$ (See Figures 1 - 3). Because these features of the free energy and the stress response change at the temperatures θ_* and θ^*, we call θ_* and θ^* the lower and upper transition temperatures, respectively.

Noting (3.17), one may easily show that the special version of the Baker-Ericksen inequalities (3.15), or equivalently (3.16), fails for $\theta \in [\bar{\theta}_*,\bar{\theta}^*]$ where

$$\begin{aligned} \bar{\theta}_*/\theta_0 &= 1 - \frac{1}{m}\sqrt{1 - \frac{ln(4/3)}{2ln(\beta_0/\alpha)}}\,, \\ \bar{\theta}^* &= 2\theta_0 - \bar{\theta}_*. \end{aligned} \tag{3.28}$$

Note that the existence of $\bar{\theta}_*$ and $\bar{\theta}^*$ is guaranteed by (3.20). By (3.24), (3.28) and (3.20), we have

$$0 < \theta_* < \bar{\theta}_* < \theta_0 < \bar{\theta}^* < \theta^*. \tag{3.29}$$

We now investigate the invertibility of the shear stress response function $\hat{\tau}(\cdot,\theta)$. By (3.27), there exist functions Γ_1, Γ_2 and Γ_3 such that

$$\begin{aligned} \Gamma_1(\hat{\tau}(\gamma,\theta),\theta) &= \gamma, \qquad for\ (\gamma,\theta) \in A_1; \\ \Gamma_2(\hat{\tau}(\gamma,\theta),\theta) &= \gamma, \qquad for\ (\gamma,\theta) \in \bar{A}_2; \\ \Gamma_3(\hat{\tau}(\gamma,\theta),\theta) &= \gamma, \qquad for\ (\gamma,\theta) \in A_3; \end{aligned} \tag{3.30}$$

with continuities:

$$\begin{aligned} &\Gamma_1(\tau_M(\theta),\theta) = \Gamma_2(\tau_M(\theta),\theta) = \gamma_M(\theta), \quad for\ \theta \in [\theta_*,\theta^*], \\ &\Gamma_2(\tau_m(\theta),\theta) = \Gamma_3(\tau_m(\theta),\theta) = \gamma_m(\theta), \quad for\ \theta \in [\theta_*,\theta^*], \\ &\Gamma_1(\hat{\tau}(\gamma,\theta_*),\theta_*) = \Gamma_3(\hat{\tau}(\gamma,\theta_*),\theta_*), \qquad for\ \gamma \geq \alpha, \\ &\Gamma_1(\hat{\tau}(\gamma,\theta^*),\theta^*) = \Gamma_3(\hat{\tau}(\gamma,\theta^*),\theta^*), \qquad for\ \alpha \geq \gamma \geq 0, \end{aligned} \tag{3.31}$$

Here the functions $\tau_m(\theta)$ and $\tau_M(\theta)$ are defined on $[\theta_*,\theta^*]$ by

$$\tau_m(\theta) = \hat{\tau}(\gamma_m(\theta), \theta), \quad \tau_M(\theta) = \hat{\tau}(\gamma_M(\theta), \theta). \tag{3.32}$$

From (3.32), (3.31) and (3.26), one can see that

$$\begin{aligned} &\tau_M(\theta) > \tau_m(\theta), \qquad for\ \theta \in (\theta_*, \theta^*); \\ &\tau_M(\theta) = \tau_m(\theta), \qquad for\ \theta = \theta_*\ or\ \theta^*. \end{aligned} \tag{3.33}$$

For each fixed θ in (θ_*, θ^*), there is a number $\tau_c(\theta)$ such that

$$\tau_m(\theta) < \tau_c(\theta) < \tau_M(\theta), \tag{3.34}$$

and

$$\int_{\Gamma_1(\tau_c(\theta),\theta)}^{\Gamma_3(\tau_c(\theta),\theta)} \hat{\tau}(\gamma, \theta)\, d\gamma = \tau_c(\theta)[\Gamma_3(\tau_c(\theta), \theta) - \Gamma_1(\tau_c(\theta), \theta)], \tag{3.35}$$

$\tau_c(\theta)$ is the so-called Maxwell stress at the temperature θ. By (3.34), (3.33), (3.32), (3.26), (3.24) and (3.18),

$$\begin{aligned} &\lim_{\theta \to \theta_* +} \tau_c(\theta) = \tau_m(\theta_*) = \tau_M(\theta_*) = \hat{\tau}(\alpha, \theta_*), \\ &\lim_{\theta \to \theta^* -} \tau_c(\theta) = \tau_m(\theta^*) = \tau_M(\theta^*) = \hat{\tau}(\alpha, \theta^*). \end{aligned} \tag{3.36}$$

To characterize a thermoelastic material completely, we must also specify the heat conductivity k defined by (2.44). From here on, we assume that

$$k(\gamma, \theta) = k_i(\theta), \qquad for\ (\gamma, \theta) \in A_i, \quad i = 1, 2, 3, \tag{3.37}$$

where $k_i(\cdot)$ are positive-valued functions and

$$k_1(\theta) \neq k_2(\theta) \neq k_3(\theta) \neq k_1(\theta), \qquad for\ \theta \in (\theta_*, \theta^*) \tag{3.38}$$

4. Equilibrium of an annular cylinder in anti-plane shear

In [14], Sammis and Dein describe a simple experiment intended to illustrate the role of phase transformations in producing large strains and creep ("superplasticity") in solids. Their interest in this issue was motivated by the possibility that superplastic behavior in the earth's mantle might arise from thermo-mechanically induced phase transformations.

The experiment of Sammis and Dein involves an annular cylindrical crystal of cesium chloride (see Fig.4) whose outer cylindrical surface is clamped and maintained at a uniform high temperature. The inner cylindrical boundary is attached to a glass tube through which cold water flows for the purpose of maintaining the inner wall at a uniform low temperature. A weight is hung from the end of the glass tube to provide an axial traction on the inner wall. The specimen is thus subject to both a mechanical load and a temperature gradient. For outer wall temperatures below a certain critical value, the crystal responds in a conventional thermoelastic manner, with the inner surface displaced axially by definite amount that depends on the size of the axial load and the temperature gradient. When the temperature at the outer wall exceeds the critical value, a phase transformation from body-centered to face-centered cubic crystal structure is initiated at the outer wall, and the interface between the two phases moves radially inward. While the phase boundary is moving, the weight attached to the central glass cooling tube experiences substantial axial creep, a phenomenon that would not occur if the response were that of a conventional thermoelastic material. Sammis and Dein measured the axial creep rate at the inner wall as a function of time for both subcritical and supercritical outer wall temperatures. In the subcritical case, very low creep rates were observed, consistent with expectations based on conventional thermoelastic response. In contrast, much larger creep rates were observed when the outer wall temperature exceeded the critical value.

Our next objective is to formulate a problem designed to provide a simple

qualitative model for the experiment of Sammis and Dein[14]. We model the specimen in their experiment as an annular cylinder composed of a thermoelastic material in the class of materials specified in the preceding chapter. We idealize the experiment itself as one in which the annular cylinder is deformed to a state of radially symmetric, finite anti-plane shear in the presence of differing inner and outer surface temperatures. The anti-plane shear is produced by a prescribed, uniformly distributed axial traction acting on the inner surface. After formulating the corresponding equilibrium boundary value problem, we construct all radially symmetric weak solutions involving at most a single surface of discontinuity of strain or temperature gradient, which we call an equilibrium shock. In Chapters 5 and 6, we discuss quasi-static anti-plane shear motions of the annular cylinder, and in Chapter 7 we determine the corresponding dissipative macroscopic response. A qualitative comparison of the creep rates observed by Sammis and Dein with the results predicted by the present model is carried out in Chapter 8.

Chapter 9 is devoted to an illustration of the shape-memory effect in the context of the model put forward here.

4.1 Formulation and reduction of the problem

Let the open reference cross-section D be the region bounded by two concentric circles of radii a and b (a < b; see Fig. 5). The temperatures on the inner wall and outer wall of the cylinder are both specified constants. Let the outer wall be fixed, and let the axial shear traction acting on the inner wall be given. Thus, the boundary conditions are given by

$$\theta = \theta_a, \qquad \sigma_{r3} = -\frac{T}{2\pi a} \qquad \textit{where } r = a, \tag{4.1}$$

$$\theta = \theta_b, \qquad u_3 = 0 \qquad \textit{where } r = b. \tag{4.2}$$

Here r, ϕ and x_3 form a cylindrical coordinate system, and the constant T is the resultant force per unit axial length acting on the inner wall. We consider radially symmetric anti-plane shear displacement and temperature that are independent of time:

$$u = u(r), \qquad \theta = \theta(r) \qquad on\ D \tag{4.3}$$

We suppose the body to be composed of the thermoelastic material described by (3.1) and (3.17) in Chapter 3. Hence, in the absence of body force, the in-plane equilibrium equations (2.40) are satisfied automatically and the out-of-plane equilibrium equation (2.41) may be integrated to give

$$\hat{\tau}(\gamma(r), \theta(r)) = \frac{T}{2\pi r}, \qquad r \in [a, b], \tag{4.4}$$

where $\hat{\tau}$ is given by (3.6). The energy equation (2.43) reduces to

$$k(\gamma(r), \theta(r)) \frac{d\theta(r)}{dr} = \frac{q_0}{2\pi r}, \qquad r \in [a, b], \tag{4.5}$$

where q_0 stands for the constant value of heat flux in the cylinder. Using (2.10) and (2.12), one can show that the heat flux must be continuous across an equilibrium shock, so that q_0 is independent of r.

The system of governing equations consists of the two first-order nonlinear ordinary differential equations (4.4) and (4.5) in the unknowns u and θ. Because of the assumed symmetry, the shock must be a cylindrical surface at, say, r = s. For simplicity, we restrict attention to the case for which

$$\theta_a \leq \theta_b, \qquad \theta_a < \theta_*; \tag{4.6}$$

other cases can be treated similarly.

4.2 Temperature distribution

Under the restriction $(4.6)_2$, Equation (3.37) gives

$$k(\gamma(r),\theta(r)) = k_1(\theta(r)), \qquad r \in (a,s). \tag{4.7}$$

For $r \in (s,b)$, however, there are three mutually exclusive possibilities (see Fig. 1 for the sets A_i, $i = 1,\ 2,\ 3$) :

$$(\gamma,\theta) \in A_i, \qquad i = 1,\ 2,\ 3. \tag{4.8}$$

By (3.37), this means

$$k(\gamma(r),\theta(r)) = k_i(\theta(r)), \qquad r \in (s,b), \qquad i = 1,\ 2,\ 3. \tag{4.9}$$

Equations(4.5) and (4.9) together with $(4.2)_1$ give

$$r = b\ exp[2\pi F_i(\theta)/q_0], \qquad r \in [s,b], \qquad i = 1,\ 2,\ 3, \tag{4.10}$$

where

$$F_i(\theta) = \int_{\theta_b}^{\theta} k_i(\phi)\ d\phi, \qquad i = 1,\ 2,\ 3. \tag{4.11}$$

Since $k_i(\cdot)$, i =1, 2, 3, are positive-valued functions, (4.10) can be inverted for i =1, 2, 3, respectively, to give

$$\theta = \hat{\theta}_i(r), \qquad r \in [s,b], \qquad i = 1,\ 2,\ 3. \tag{4.12}$$

Similarly, from (4.5), (4.7) and $(4.1)_1$, one has

$$r = a\ exp\{2\pi[F_1(\theta) - F_1(\theta_a)]/q_0\}, \quad r \in [a,s], \tag{4.13}$$

which can be inverted to give

$$\theta = \hat{\theta}_0(r), \qquad r \in [a,s]. \tag{4.14}$$

For each choice of i in (4.12), continuity of temperature requires

$$\hat{\theta}_i(s) = \hat{\theta}_0(s), \qquad i = 1,\ 2,\ 3, \tag{4.15}$$

this leads to the determination of the heat flux, $q_0 = \hat{q}_i(s)$, $i = 1, 2, 3$.
For convenience, define

$$\Theta_i(r; s, \theta_b) = \begin{cases} \hat{\theta}_0(r), & r \in [a, s]; \\ \hat{\theta}_i(r), & r \in [s, b], \end{cases} \qquad i = 1,\ 2,\ 3. \tag{4.16}$$

Here, we explicitly exhibit both s and θ_b as parameters, because we shall allow them to change in later chapters. In fact, one can readily show that $\Theta_1(r; s, \theta_b)$ is independent of s.

Note that in the case of $\theta_b \leq \theta_*$, we have i = 1, and there is no possibility of mixed-phase equilibrium. To obtain a mixed-phase equilibrium, we assume that

$$\theta_b > \theta_*. \tag{4.17}$$

Since

$$k(\cdot, \theta) \equiv k_1(\theta), \qquad for\ \ \theta \leq \theta_*, \tag{4.18}$$

we must have

$$\Theta_i(s; s, \theta_b) \geq \theta_*, \qquad i = 2,\ 3. \tag{4.19}$$

Thus corresponding to each Θ_i, i = 2, 3, s has a lower bound r_i^* which is defined by

$$\Theta_i(r_i^*; r_i^*, \theta_b) = \theta_*, \qquad i = 2,\ 3. \tag{4.20}$$

For future use, we define functions $\hat{r}_i^*(\cdot)$ on [r_i^*,b] by

$$\Theta_i(\hat{r}_i^*(s); s, \theta_b) = \theta_*, \qquad i = 2,\ 3. \tag{4.21}$$

One can show that

$$\hat{r}_i^*(r_i^*) = r_i^*, \qquad \hat{r}_i^*(b) = r_1^*, \qquad i = 2,\ 3, \tag{4.22}$$

where r_1^* is defined by

$$\Theta_1(r_1^*, r_1^*, \theta_b) = \theta_*. \tag{4.23}$$

4.3 Displacement field

For, $r \in (s, b)$, there are three mutually exclusive possibilities corresponding to (4.8), which, together with (3.30), yield the strain γ(r) as either

$$\gamma(r) = \Gamma_1(\frac{T}{2\pi r}, \Theta_1(r; s, \theta_b)), \quad for\ r \in (s, b), \tag{4.24}$$

or

$$\gamma(r) = \Gamma_2(\frac{T}{2\pi r}, \Theta_2(r; s, \theta_b)), \quad for\ r \in (s, b), \tag{4.25}$$

or

$$\gamma(r) = \Gamma_3(\frac{T}{2\pi r}, \Theta_3(r; s, \theta_b)), \quad for\ r \in (s, b). \tag{4.26}$$

Similarly, we have either

$$\gamma(r) = \Gamma_1(\frac{T}{2\pi r}, \Theta_1(r; s, \theta_b)), \quad for\ r \in (a, s), \tag{4.27}$$

or

$$\gamma(r) = \Gamma_1(\frac{T}{2\pi r}, \Theta_2(r; s, \theta_b)), \quad for\ r \in (a, s), \tag{4.28}$$

or

$$\gamma(r) = \Gamma_1(\frac{T}{2\pi r}, \Theta_3(r; s, \theta_b)), \quad for\ r \in (a, s). \tag{4.29}$$

Combining (4.24) with (4.27), we get

$$\gamma(r) = \Gamma_1(\frac{T}{2\pi r}, \Theta_1(r; s, \theta_b)), \quad for\ r \in (a, b), \tag{4.30}$$

Recalling (3.25) and (3.30), we infer from (4.30) that

$$T \le T_1^M(r,s,\theta_b), \qquad \forall r \in [r_1^*, b], \tag{4.31}$$

where

$$T_1^M(r,s,\theta_b) = 2\pi r \tau_M(\Theta_1(r;s,\theta_b)) = T_1^M(r,b,\theta_b), \quad \forall r \in [r_1^*, b]. \tag{4.32}$$

Equations (4.30) and $(4.2)_2$ give

$$u(r) = U_1(r;s,T,\theta_b) = -\int_r^b \Gamma_1(\frac{T}{2\pi x}, \Theta_1(x;s,\theta_b))\, dx, \quad r \in [a,b]. \tag{4.33}$$

If (4.25) and (4.28) hold, we have

$$\begin{aligned} T \le & T_2^M(r,s,\theta_b), \quad r \in (\hat{r}_2^*(s), s], \\ T_2^m(r,s,\theta_b) \le & T \le T_2^M(r,s,\theta_b), \quad r \in [s,b], \end{aligned} \qquad s \in [r_2^*, b], \tag{4.34}$$

where

$$\begin{aligned} T_2^M(r,s,\theta_b) &= 2\pi r \tau_M(\Theta_2(r;s,\theta_b)), \\ T_2^m(r,s,\theta_b) &= 2\pi r \tau_m(\Theta_2(r;s,\theta_b)), \end{aligned} \qquad r \in [\hat{r}_2^*(s), b],\ s \in [r_2^*, b]. \tag{4.35}$$

Equations (4.25) and (4.28), together with $(4.2)_2$, give the out-of-plane displacement

$$u(r) = U_2(r;s,T,\theta_b)$$
$$= \begin{cases} -[\int_r^s \Gamma_1(\frac{T}{2\pi x}, \Theta_2(x;s,\theta_b))\, dx + \int_s^b \Gamma_2(\frac{T}{2\pi x}, \Theta_2(x;s,\theta_b))\, dx], & r \in [a,s]; \\ -\int_r^b \Gamma_2(\frac{T}{2\pi x}, \Theta_2(x;s,\theta_b))\, dx, & r \in [s,b]. \end{cases} \tag{4.36}$$

Finally, the validity of (4.26) and (4.29) requires

$$\begin{aligned} & T \le T_3^M(r,s,\theta_b), \quad r \in (\hat{r}_3^*(s), s], \quad s \in (r_3^*, b]; \\ & T \ge T_3^m(r,s,\theta_b), \quad r \in [s,b], \quad s \in [r_3^*, b), \end{aligned} \tag{4.37}$$

where

$$\begin{aligned} T_3^M(r,s,\theta_b) &= 2\pi r \tau_M(\Theta_3(r;s,\theta_b)) \\ T_3^m(r,s,\theta_b) &= 2\pi r \tau_m(\Theta_3(r;s,\theta_b)) \end{aligned} \qquad r \in [\hat{r}_3^*(s), b], \quad s \in [r_3^*, b]. \tag{4.38}$$

Equations (4.26) and (4.29) together with $(4.2)_2$ give

$$u(r) = U_3(r; s, T, \theta_b)$$

$$= \begin{cases} -[\int_r^s \Gamma_1(\frac{T}{2\pi x}, \Theta_3(x; s, \theta_b))\, dx + \int_s^b \Gamma_3(\frac{T}{2\pi x}, \Theta_3(x; s, \theta_b))\, dx], & r \in [a, s]; \\ -\int_r^b \Gamma_3(\frac{T}{2\pi x}, \Theta_3(x; s, \theta_b))\, dx, & r \in [s, b]. \end{cases} \tag{4.39}$$

4.4 Non-uniqueness of the equilibrium states

As we have seen in the previous section, the equilibrium problem under consideration does not have unique solution for given T, θ_a and θ_b in general. To examine the totality of solutions, we introduce the following sets in the s,T-plane for fixed θ_b:

$$\begin{aligned} \Sigma_1(\theta_b) &= \{(s,T)/ \quad T \le T_1(\theta_b), \quad s = b\}, \\ \Sigma_2(\theta_b) &= \{(s,T)/ \quad T_2^m(s,\theta_b) \le T \le T_2^M(s,\theta_b), \quad s \in [r_2^*, b]\}, \\ \Sigma_3(\theta_b) &= \left\{ (s,T)/ \begin{array}{ll} T \le T_3^M(s,\theta_b), & s \in (r_3^*, b]; \\ T \ge T_3^m(s,\theta_b), & s \in [r_3^*, b] \end{array} \right\}, \end{aligned} \tag{4.40}$$

where

$$\begin{aligned} T_1(\theta_b) &= \min_{r \in [r_1^*, b]} \{T_1^M(r, b, \theta_b)\}, \\ T_2^M(s,\theta_b) &= \inf_{r \in (f_2^*(s), b]} \{T_2^M(r, s, \theta_b)\}, \\ T_3^M(s,\theta_b) &= \inf_{r \in (f_3^*(s), s]} \{T_3^M(r, s, \theta_b)\}, \\ T_i^m(s,\theta_b) &= \max_{r \in [s, b]} \{T_i^m(r, s, \theta_b)\}, \quad i = 2,\ 3. \end{aligned} \tag{4.41}$$

From (4.31)-(4.41), we conclude that a pair of functions $\Theta_i(\cdot; s, \theta_b)$ and $U_i(\cdot; s, T, \theta)$ is a solution of our problem if and only if (s,T) belongs to $\Sigma_i(\theta_b)$, i = 1, 2, 3. Let $\Im_i$, i = 1, 2, 3, denote the corresponding three classes of solutions as follows

$$\Im_i = \{\theta_i(\cdot; s, \theta_b), U_i(\cdot; s, T, \theta_b) / \quad (s,T) \in \Sigma_i(\theta_b), \quad \forall \theta_b \in [\theta_*, \theta^*]\}, \qquad i = 1,\ 2,\ 3. \tag{4.42}$$

The solutions in $\Im_1$ are independent of the shock position s; we will consider these solutions as $s = b$. Then, for given T and θ_b appropriately, we have a solution in $\Im_1$, a one-parameter family of solutions in $\Im_2$ with the parameter s, $r_2^* \le s \le b$, and a one-parameter family of solutions in $\Im_3$ with the parameter s, $r_3^* \le s \le b$. For qualitative purposes, these are shown schematically in Fig. 6.

From Fig. 6, one can draw the following conclusions:

(a) $\theta_* < \theta_b \le \bar{\theta}_*$:

For a load T such that	there exist
$0 \le T \le T_2^m(b, \theta_b)$	a unique solution which is smooth;
$T_2^m(b, \theta_b) < T \le T_1(\theta_b)$	two one-parameter families of solutions, one smooth solution;
$T_1(\theta_b) < T < T_*$	a one-parameter family of solutions, no smooth solutions;
$T_* \le T < \infty$ (here $T_* = 2\pi r_3^* \tau_M(\theta_*)$).	a unique solution;

(b) $\bar{\theta}_* < \theta_b < \bar{\theta}^*$:

For a load T such that	there exist
$0 \le T \le T_1(\theta_b)$	two one-parameter families of solutions, one smooth solution;
$T_1(\theta_b) < T < T_*$	a one-parameter family of solutions, no smooth solutions;
$T_* \le T < \infty$	a unique solution.

For sufficiently large load ($T > T_*$), the solution involves a smooth displacement field u, but the temperature field θ is not smooth unless

$$k_1(\theta_*) = k_3(\theta_*). \tag{4.43}$$

For $\bar{\theta}^* \leq \theta_b \leq \theta^*$, the result is similar to that described in Fig. 6(a) if we only consider solutions involving at most a single shock, or phase boundary. However, in the case $\theta_b \geq \theta^*$, it may be necessary to consider solutions involving multiple shocks.

5. Quasi-static motions and admissibility

5.1 Quasi-static motions

Here we consider quasi-static motions in which, at each instant, the state (θ,u) is in equilibrium and belongs to the collection:

$$\Im = \Im_1 \cup \Im_2 \cup \Im_3. \tag{5.1}$$

Let $L \equiv [t_0, t_1]$ be a finite time interval, and let Λ be a mapping of L into $\Im$; thus there are two functions $\theta(\cdot, t)$ and $u(\cdot, t)$ defined on [a,b] and such that

$$\Lambda(t) = (\theta(\cdot, t), u(\cdot, t)), \quad (\theta(\cdot, t), u(\cdot, t)) \in \Im, \quad t \in L. \tag{5.2}$$

Every mapping Λ determines a unique quadruple of functions $i(\cdot), s(\cdot), T(\cdot)$ and $\theta_b(\cdot)$ on L such that

$$i(t) = 1,\ 2 \text{ or } 3 \quad \textit{and} \quad (s(t), T(t)) \in \Sigma_{i(t)}(\theta_b(t)), \quad t \in L, \tag{5.3}$$

and

$$\begin{aligned} \theta(\cdot, t) &= \Theta_{i(t)}(\cdot; s(t), \theta_b(t)), \\ u(\cdot, t) &= U_{i(t)}(\cdot; s(t), T(t), \theta_b(t)), \end{aligned} \qquad t \in L. \tag{5.4}$$

The mapping Λ is a quasi-static motion if the associated quadruple has the following properties:

(a) $i(\cdot)$ is piecewise constant on L, taking one of three values 1, 2, 3 at each instant t;

(b) $s(\cdot)$, $T(\cdot)$ and $\theta_b(\cdot)$ are continuous and piecewise continuously differentiable on L, and $(s(t), T(t)) \in \Sigma_{i(t)}(\theta_b(t))$, $\forall t \in L$;

(c) $\theta(r, \cdot)$ and $u(r, \cdot)$ are both continuous on L for every $r \in [a, b]$.

An instant $t_* \in L$ at which $i(t)$ is discontinuous is called a transition instant.

Proposition 5.1: Let $i(\cdot)$, $s(\cdot)$, $T(\cdot)$ and $\theta_b(\cdot)$ be functions on L with properties (a) and (b) above. Define $\theta(\cdot,\cdot)$ and $u(\cdot,\cdot)$ on $[a,b] \times L$ by (5.4). Then θ and u have property (c) if and only if, at every transition instant $t_* \in L$,

$$s(t_*) = b. \tag{5.5}$$

Proof: Suppose first that (c) holds, so that $\theta(r,\cdot)$ is continuous on L. Then by (5.4), if t_* is a transition instant in (t_0, t_1),

$$\lim_{t \to t_*-} \Theta_{i(t)}(r; s(t), \theta_b(t)) = \lim_{t \to t_*+} \Theta_{i(t)}(r; s(t), \theta_b(t)), \quad r \in [a,b]. \tag{5.6}$$

There is a $\delta > 0$ such that $i(\cdot)$ is continuous on $(t_* - \delta, t_* + \delta)$ except at t_*, so that (5.6) implies

$$\Theta_j(r; s, \theta_b) = \Theta_k(r; s, \theta_b), \qquad r \in [a,b], \tag{5.7}$$

where $j = i(t_*-)$, $k = i(t_*+)$, $s = s(t_*)$, $\theta_b = \theta_b(t_*)$. By (4.16), (5.7) is equivalent to

$$\hat{\theta}_0(r; \hat{q}_j(s)) = \hat{\theta}_0(r; \hat{q}_k(s)), \qquad a \le r \le s, \tag{5.8}$$

$$\hat{\theta}_j(r; \hat{q}_j(s)) = \hat{\theta}_k(r; \hat{q}_k(s)), \qquad s \le r \le b. \tag{5.9}$$

By (4.5), (5.8) implies

$$\hat{q}_j(s) = \hat{q}_k(s), \qquad at\ s = s(t_*). \tag{5.10}$$

From (4.5), (5.9) and (5.10), it follows that

$$k_j(\theta) = k_k(\theta), \quad \theta(s(t_*), t_*) \le \theta \le \theta_b. \tag{5.11}$$

Since t_* is a point of discontinuity of $i(\cdot)$, one has $j \neq k$. Hence (5.11) contradicts (3.38) unless (5.5) holds. Minor modifications of the above argument can be used

to deal with the case $t_* = t_0$ and $t_* = t_1$. Thus property (c), in the presence of properties (a) and (b), implies (5.5).

Next we prove that $\theta(r,\cdot)$ and $u(r,\cdot)$ are both continuous on L for every $r \in [a,b]$ under the assumption that (5.5) holds at every transition instant $t_* \in L$. Note that continuity of $\theta(r,\cdot)$ and $u(r,\cdot)$ at any non-transition instant for every $r \in [a,b]$ follows from the continuity of $s(\cdot)$, $T(\cdot)$ and $\theta_b(\cdot)$ as guaranteed by property (b). At a transition instant $t_* \in L$, by property (a) and (5.5), (5.4) yields

$$\lim_{t \to t_*-} (\theta(r,t), u(r,t)) = (\Theta_j(r; b, \theta_b), U_j(r; b, T, \theta_b)), \quad r \in [a,b], \tag{5.12}$$

and

$$\lim_{t \to t_*+} (\theta(r,t), u(r,t)) = (\Theta_k(r; b, \theta_b), U_k(r; b, T, \theta_b)), \quad r \in [a,b], \tag{5.13}$$

where $j = i(t_*-)$, $k = i(t_*+)$ and $T = T(t_*)$, $\theta_b = \theta_b(t_*)$. By the analysis in the previous chapter, one has

$$\begin{aligned} (\Theta_i(r; b, \theta_b), U_i(r; b, T, \theta_b)) = (\Theta_1(r; b, \theta_b), U_1(r; b, T, \theta_b)) \\ r \in [a,b], \quad i = 1,\ 2,\ 3. \end{aligned} \tag{5.14}$$

Hence $\theta(r,\cdot)$ and $u(r,\cdot)$ are continuous at a transition instant and therefore at all instants in L. Thus (5.5), in the presence of properties (a) and (b), implies property (c), and the proposition is established.

5.2 Admissibility

For quasi-static motions in the annular cylinder problem, Equation (2.20) which is a consequence of the second law of thermodynamics reduces to[1]

[1] Here the normal **N** is chosen towards the inner wall of the annular cylinder.

$$-f(s(t),t)\dot{s}(t) \geq 0, \qquad t \in L, \tag{5.15}$$

where the driving traction f is given by

$$f(s,t) = h_{i(t)}(\frac{T(t)}{2\pi s}, \theta(s,t)), \tag{5.16}$$

and $h_j(\cdot,\cdot)$ are the material functions defined by

$$\begin{aligned} h_j(\tau,\theta) =& \Psi(\Gamma_1(\tau,\theta),\theta) - \Psi(\Gamma_j(\tau,\theta),\theta) - \tau[\Gamma_1(\tau,\theta) - \Gamma_j(\tau,\theta)], \\ & for\ \tau_m(\theta) \leq \tau \leq \tau_M(\theta), \quad \theta_* < \theta < \theta^*, \quad j = 1,\ 2,\ 3, \end{aligned} \tag{5.17}$$

where Ψ is defined by (3.21).

We will say a quasi-static motion is admissible if (5.15) holds.

By the definitions (5.17) and (3.30) of h_j and Γ_j, one can see that $h_1(\cdot,\cdot)$ vanishes identically, and that

$$\begin{aligned} \frac{\partial h_j(\tau,\theta)}{\partial \tau} =& \Gamma_j(\tau,\theta) - \Gamma_1(\tau,\theta), \qquad j = 2,\ 3, \\ & for\ \tau_m(\theta) < \tau < \tau_M(\theta), \quad \theta \in (\theta_*,\theta^*). \end{aligned} \tag{5.18}$$

Recalling the definition in Chapter 3 of the Maxwell stress $\tau_c(\theta)$ and noting that $\Gamma_2(\tau_M(\theta),\theta) = \Gamma_1(\tau_M(\theta),\theta) = \gamma_M(\theta)$ for $\theta \in [\theta_*,\theta^*]$, one can show that

$$\begin{aligned} h_2(\tau,\theta) &= -\int_{\tau}^{\tau_M(\theta)} [\Gamma_2(\sigma,\theta) - \Gamma_1(\sigma,\theta)]\, d\sigma, \\ h_3(\tau,\theta) &= \int_{\tau_c(\theta)}^{\tau} [\Gamma_3(\sigma,\theta) - \Gamma_1(\sigma,\theta)]\, d\sigma, \\ & for\ \tau_m(\theta) \leq \tau \leq \tau_M(\theta), \quad \theta \in (\theta_*,\theta^*). \end{aligned} \tag{5.19}$$

Therefore, we have the following proposition:

Proposition 5.2: Let Λ be a quasi-static motion on L. If, at some instant $t \in L$, $\Lambda(t) \in \Im_2$, then the admissibility condition (5.15) requires that either

$$\dot{s}(t) \geq 0, \tag{5.20}$$

or

$$f(s(t), t) = 0. \tag{5.21}$$

This proposition follows immediately from (5.15), (5.16) and $(5.19)_1$.

As a consequence of the admissibility, the next proposition excludes the possibility that a particle transforms to phase 2 from either phase 1 or phase 3.

Proposition 5.3: Let Λ be an admissible quasi-static motion on L. If at some instant $t' \in [t_0, t_1)$, $\Lambda(t') \in \Im_1 \cup \Im_3$, then $\Lambda(t) \in \Im_1 \cup \Im_3$ for any instant $t \in [t', t_1]$.

Proof: Suppose the result of the proposition is false. Then there exists an admissible quasi-static motion Λ on L such that

$$\Lambda(t') \in \Im_1 \cup \Im_3, \qquad \Lambda(t'') \in \Im_2, \tag{5.22}$$

where

$$t' < t'', \qquad [t', t''] \subset L. \tag{5.23}$$

Since $\Lambda(t'') \in \Im_2$ implies that $s(t'') < b$, by Proposition 5.1, there exists a finite interval $[t_*, t_2] \subset [t', t'']$ where t_* is a transition instant such that

$$\begin{cases} \dot{s}(t) < 0, & \text{for } t_* \leq t \leq t_2, \\ \Lambda(t) \in \Im_2, & \text{for } t_* < t \leq t_2. \end{cases} \tag{5.24}$$

Hence Proposition 5.2 requires that the driving traction $f(s(\cdot), \cdot)$ vanish identically on $[t_*, t_2]$ which, by (5.16) and $(5.19)_1$, implies that

$$\frac{T(t)}{2\pi s(t)} = \tau_M(\theta(s(t), t)), \quad \forall\, t \in [t_*, t_2], \tag{5.25}$$

i.e.

$$\Gamma_1(\frac{T(t)}{2\pi s(t)}, \theta(s(t), t)) = \Gamma_2(\frac{T(t)}{2\pi s(t)}, \theta(s(t), t)) = \gamma_M(\theta(s(t), t)), \quad \text{for } t \in [t_*, t_2]. \tag{5.26}$$

Noting that

$$\frac{\partial \hat{\tau}(\gamma,\theta)}{\partial \gamma} = 0, \quad for\ \gamma = \gamma_M(\theta), \quad \theta \in [\theta_*, \theta^*], \tag{5.27}$$

one finds from (4.4) and (4.5) that

$$\begin{gathered} \lim_{r\to s(t)-} \frac{\partial \theta}{\partial r}(r,t) = \lim_{r\to s(t)+} \frac{\partial \theta}{\partial r}(r,t), \\ \lim_{r\to s(t)-} [f_1(\theta(r,t))\frac{\partial \theta}{\partial r}(r,t)] = \lim_{r\to s(t)+} [f_2(\theta(r,t))\frac{\partial \theta}{\partial r}(r,t)], \\ for\ \ t_* \le t \le t_2. \end{gathered} \tag{5.28}$$

By (3.38), Equation(5.28) holds only if

$$\theta(s(t),t) = \theta_*, \quad \forall t \in [t_*, t_2], \tag{5.29}$$

which implies that

$$\theta_* = \lim_{t\to t_*+} \theta(s(t),t) = \theta(b,t_*) = \theta_b(t_*). \tag{5.30}$$

This contradicts the assumption made in (4.17), establishing the proposition.

According to Proposition 5.3, an admissible quasi-static motion that begins in either phase one ($\Im_1$) or phase three ($\Im_3$) can never enter phase two ($\Im_2$). In particular, quasi-static motions that commence at the undeformed state can never enter phase two. We thus exclude states in $\Im_2$ from here on. Recalling the definitions (4.16), (4.33) and (4.39) of Θ_i, U_1 and U_3, one can show that

$$\begin{gathered} [\Theta_1(\cdot;b,\theta_b), U_1(\cdot;b,T,\theta_b)] \equiv [\Theta_3(\cdot;b,\theta_b), U_3(\cdot;b,T,\theta_b)], \\ for \quad T \le T_1(\theta_b). \end{gathered} \tag{5.31}$$

Noting the definitions (4.40) and (4.42) of $f_i(\theta_b)$ and $\Im_i$, one can write

$$\Im_1 = \{\theta_3(\cdot;s,\theta_b), U_3(\cdot;s,T,\theta_b) / \quad (s,T) \in \Sigma_1(\theta_b)\}. \tag{5.32}$$

Thus, for any quasi-static motion that begins in either phase one ($\Im_1$) or phase three ($\Im_3$), we have

$$\begin{aligned} \theta(r,t) &= \Theta_3(r; s(t), \theta_b(t)), \\ u(r,t) &= U_3(r; s(t), T(t), \theta_b(t)), \end{aligned} \qquad \forall\,(r,t) \in [a,b] \times L. \tag{5.33}$$

Hence, when the load T(t) and the temperature $\theta_b(t)$ on the outer wall are given, the temperature field $\theta(\cdot,t)$ and the displacement field $u(\cdot,t)$ for each instant $t \in L$ are determined by (5.33) uniquely up to an unknown function $s(\cdot)$ which specifies the location of the shock, or phase boundary, at every instant. As pointed out by Abeyaratne and Knowles [13], this suggests that some additional constitutive information concerning the kinetics of the phase transformation must be provided.

For the so-called hard device problem, the displacement $\delta(\cdot)$ on the inner wall would be specified instead of the load $T(\cdot)$. By (5.33),

$$\delta = \hat{\delta}(T; s, \theta_b) = U_3(a; s, T, \theta_b), \quad \textit{at any instant.} \tag{5.34}$$

Recalling (4.39), (3.30) and (3.22), one can show that

$$\frac{\partial \hat{\delta}}{\partial T}(T; \cdot, \cdot) < 0, \quad \textit{for all } T, \tag{5.35}$$

assuring that there is a unique inverse $\hat{T}(\cdot; s, \theta_b)$ for $\hat{\delta}(\cdot; s, \theta_b)$:

$$T = \hat{T}(\delta; s, \theta_b) \tag{5.36}$$

for all δ, and for appropriate values of s and θ_b.

Define

$$\begin{aligned} \hat{U}(r; s, \delta, \theta_b) &= U_3(r; s, \hat{T}(\delta; s, \theta_b), \theta_b), \\ &\textit{for } r \in [a,b],\ s \in [r_3^*, b],\ \delta \geq 0,\ \theta_b \geq \theta_a. \end{aligned} \tag{5.37}$$

Then by (5.33),

$$\begin{aligned} \theta(r,t) &= \Theta_3(r; s(t), \theta_b(t)), \\ u(r,t) &= \hat{U}(r; s(t), \delta(t), \theta_b(t)), \end{aligned} \qquad \forall\,(r,t) \in [a,b] \times L. \tag{5.38}$$

Again, the quasi-static motion is described by (5.38) uniquely up to an unknown function $s(\cdot)$.

6. Completion of constitutive assumptions

As we have seen in Chapter 5, additional constitutive information is needed in order to determine the location of the phase boundary during quasi-static motions. One may view this constitutive deficiency as arising from the fact that the constitutive relations (2.21) - (2.24) are not meaningful on the phase boundary. In this chapter, we complete the constitutive description of the material by specifying a kinetic relation that controls the rate at which the phase transformation takes place, and a transformation strain that determines the onset of the transformation.

6.1 The kinetic relation

As in the work of Abeyaratne and Knowles [13] on modeling phase transformations in the setting of finite elasticity, we assume that the normal component of the propagation velocity of phase boundary depend on the driving traction and the temperature on the phase boundary. Thus we suppose that there exists a function $\hat{V}(\cdot,\theta)$ for $\theta \in [\theta_*, \theta^*]$ such that

$$V_N(\mathbf{x},t) = \hat{V}(f(\mathbf{x},t),\theta(\mathbf{x},t)), \quad for\ \mathbf{x} \in S(t),\ t \in L. \tag{6.1}$$

For the annular cylinder problem, we have shown, in the previous chapter, that

$$f(s,t) = h(\frac{T(t)}{2\pi s},\theta(s,t)), \quad for\ (s,t) \in [a,b] \times L, \tag{6.2}$$

where $h(\cdot,\cdot)$ is a material function defined through the inverse functions Γ_3, Γ_1 of (3.30) by

$$\begin{aligned} h(\tau,\theta) &= \int_{\tau_c(\theta)}^{\tau} [\Gamma_3(\sigma,\theta) - \Gamma_1(\sigma,\theta)]\, d\sigma. \\ &for\ \tau_m(\theta) \le \tau \le \tau_M(\theta), \quad \theta \in [\theta_*, \theta^*], \end{aligned} \tag{6.3}$$

where $\tau_c(\theta)$ is the Maxwell stress at temperature θ.

Define

$$f_m(\theta) = h(\tau_m(\theta), \theta), \quad f_M(\theta) = h(\tau_M(\theta), \theta), \quad for\ \theta \in [\theta_*, \theta^*]. \tag{6.4}$$

Then by (6.3),

$$f_m(\theta) \leq h(\tau, \theta) \leq f_M(\theta), \quad for\ \tau_m(\theta) \leq \tau \leq \tau_M(\theta), \quad \theta \in [\theta_*, \theta^*]. \tag{6.5}$$

Hence in the cylinder problem, the kinetic response function $\hat{V}(\cdot, \theta)$ is to be defined on $(f_m(\theta), f_M(\theta))$ for $\theta \in [\theta_*, \theta^*]$, and the kinetic relation (6.1) specializes to

$$-\dot{s} = \hat{V}(f(s,t), \theta(s,t)), \quad for\ (s,t) \in [a,b] \times L, \tag{6.6}$$

where s(t) is the radius of the phase boundary at time t.

Concerning the form of the kinetic function (see Fig.7), we assume that $\hat{V}(\cdot, \theta)$ is continuous on $(f_m(\theta), f_M(\theta))$ for every $\theta \in (\theta_*, \theta^*)$ and that

(i) There exist two material functions $m(\theta)$ and $M(\theta)$ on (θ_*, θ^*) satisfying

$$f_m(\theta) < m(\theta) \leq 0 \leq M(\theta) < f_M(\theta), \quad for\ \theta \in (\theta_*, \theta^*), \tag{6.7}$$

and such that

$$\hat{V}(f, \theta) \begin{cases} < 0 & \text{for } f_m(\theta) < f < m(\theta); \\ = 0 & \text{for } m(\theta) \leq f \leq M(\theta); \\ > 0 & \text{for } M(\theta) < f < f_M(\theta); \end{cases} \qquad \theta \in (\theta_*, \theta^*), \tag{6.8}$$

(ii) moreover

$$\hat{V}(0, \theta) = 0, \qquad for\ \theta \in [\theta_*, \theta^*], \tag{6.9}$$

$$\lim_{f \to f_m(\theta)} \hat{V}(f,\theta) = -\infty, \quad \lim_{f \to f_M(\theta)} \hat{V}(f,\theta) = \infty, \quad for\ \theta \in (\theta_*, \theta^*). \tag{6.10}$$

Note that $m(\theta) \equiv M(\theta) \equiv 0$ is a permissible choice.

If T(t) is given and $\theta(s(t),t)$ is represented in terms of s(t) by (5.38) and (4.16), then (6.6) become an ordinary differential equation for s(t). To arrive at an appropriate initial condition for this differential equation, we need a criterion for initiation of the phase transformation, to which we now turn.

6.2 The transformation strain postulate

Define two functions $\gamma_c(\cdot)$ and $\gamma^c(\cdot)$ on $[\theta_*, \theta^*]$ by

$$\gamma_c(\theta) = \Gamma_1(\tau_c(\mathcal{J}), \theta), \quad \gamma^c(\theta) = \Gamma_3(\tau_c(\theta), \theta), \tag{6.11}$$

where $\tau_c(\theta)$ is the Maxwell stress.

Assume that there exist two material functions $\gamma_T(\cdot)$ and $\gamma^T(\cdot)$ on (θ_*, θ^*), taking values (see Fig. 8)

$$\begin{gathered} \gamma_c(\theta) < \gamma_T(\theta) \leq \gamma_M(\theta) < \gamma_m(\theta) \leq \gamma^T(\theta) < \gamma^c(\theta), \\ for\ \theta \in (\theta_*, \theta^*), \end{gathered} \tag{6.12}$$

such that

i) A particle at r = $\tilde{r}$ will "spontaneously" transform from phase-1 to phase-3 at t = $\tilde{t}$ if

$$\theta(\tilde{r},\tilde{t}) \in (\theta_*, \theta^*) \quad and \quad \gamma(\tilde{r},\tilde{t}) = \gamma_T(\theta(\tilde{r},\tilde{t})); \tag{6.13}$$

ii) A particle at r = $\tilde{r}$ will "spontaneously" transform from phase-3 to phase-1 at t = $\tilde{t}$ if

$$\theta(\tilde{r},\tilde{t}) \in (\theta_*,\theta^*) \quad \textit{and} \quad \gamma(\tilde{r},\tilde{t}) = \gamma^T(\theta(\tilde{r},\tilde{t})); \tag{6.14}$$

We may call $\gamma_T(\cdot)$ and $\gamma^T(\cdot)$ the (1,3)-transformation strain and the (3,1)-transformation strain, respectively.

7. Macroscopic thermo-mechanical responses

We now elucidate the features of the macroscopic response of the cylinder under various loading programs, with the temperature θ_b at the outer wall fixed. We shall adopt a kinetic relation of the type illustrated in Fig. 7. For convenience, we recall here from (5.34) and (5.36) the macroscopic response for soft and hard devices, respectively:

$$\delta(t) = \hat{\delta}(T(t); s(t), \theta_b(t)), \quad t_0 \leq t \leq t_1; \tag{7.1}$$

$$T(t) = \hat{T}(\delta(t); s(t), \theta_b(t)), \quad t_0 \leq t \leq t_1. \tag{7.2}$$

7.1 Hysteresis and rate-dependence

First let $T(t) = \lambda t$, corresponding to soft device loading at a constant rate λ from the undeformed state. Assume that the final value of the load T is larger than $T_*(\theta_b)$, and that the fixed value of the outer wall temperature θ_b is such that $\theta_* < \theta_b < \bar{\theta}_*$. The $T - \delta$ response is shown schematically in Fig. 9.[1] After loading begins, the point $(\delta(t), T(t))$ rises from the origin O along the response curve OAQ, associated with a single phase solution at each instant. At $t = \tilde{t}$, the point $(\delta(t), T(t))$ reaches the point Q in Fig. 9. When this occurs, the amount of shear $\gamma(b, \tilde{t})$ at the outer wall achieves the value $\gamma_T(\theta_b)$ of the (1,3)-transformation strain at the wall temperature θ_b, so that a phase transformation is initiated according to the initiation criterion (6.13), and a 1,3-phase boundary emerges at r = b. The kinetic relation (6.6) then takes over, and the phase boundary has the initial velocity $\dot{s}(\tilde{t}) = -\hat{V}(f(b, \tilde{t}), \theta_b)$. Under the control of (6.6), s(t) monotonically decreases with t until $s = r_3^*(\theta_b)$; this occurs at time $t = T_*(\theta_b)/\lambda$. The axial displacement $\delta(t)$ at the inner wall is given by (7.1), and point

[1] Here it is assumed that $\theta_* < \theta_b < \bar{\theta}_*$; this guarantees the absence of residual deformation, which is considered in the next section.

$(\delta(t), T(t))$ moves along the curve QBP. This stage of the process is accompanied by a phase transformation. As the load T(t) continues to increase, the phase boundary remains at $r = r_3^*(\theta_b)$ since the temperatures at points for which $r < r_3^*(\theta_b)$ are too low ($< \theta_*$) for the material to support a phase transformation.

Now suppose that T(t) is decreased at the constant rate λ from its largest value at the point Z in Fig. 9 to zero. The associated response curve at first follows the arc ZP, and the phase boundary stays at $r = r_3^*(\theta_b)$, so there is no reverse phase transformation at this stage. As T(t) continues to decrease, s(t) increases with time under the control of (6.6), i.e., the phase boundary moves toward the outer wall, and the point $(\delta(t), T(t))$ moves along the curve PCA. As T(t) decreases to zero from its value at A, s(t) remains at the value b until the point $(\delta(t), T(t))$ returns to the origin along the curve AO.

If we change the loading rate λ, the arcs QBP, PCA will change, but OAQ and PZ would remain the same. For different loading-unloading-reloading processes, we have different macroscopic response curves similar to those predicted by Abeyaratne and Knowles[13].

7.2 Residual defomation

If the outer wall temperature θ_b is fixed such that $\bar{\theta}_* < \theta_b < \bar{\theta}^*$, some residual deformation would be produced by the mechanical cycling process described in the previous section. In this case, the macroscopic response, during the loading period, is qualitatively the same as that sketched in the last section, but during the unloading period, it is quite different. At first the response curve (see Fig. 10) follows the arc ZP, and the phase boundary remains stationary at $r = r_3^*(\theta_b)$. When T(t) decreases to zero from $T_*(\theta_b)$, according to (6.6), the phase boundary moves towards the outer wall and arrives at $r = s_1 < b$, corresponding to the arc PCD. If the driving traction f at the phase boundary at this instant, say $t = t_1$, is less than the critical value $m(\theta(s_1, t_1))$, then the phase boundary continues to

move towards the outer wall, and the point $(\delta(t), T(t))$ "creeps" to E from D at zero load. Creep response under more general conditions will be discussed in the next chapter.

7.3 Stress relaxation

Let the outer wall temperature θ_b be fixed, with $\theta_* < \theta_b < \theta^*$. We first let $\delta(t) = \lambda t$, corresponding to hard device loading at a constant rate λ from the undeformed state. The corresponding response curve[1] is the arc OQB in Fig. 11. If we stop loading at B, subsequently keeping δ constant, the phase boundary continues to move towards the inner wall, and the point $(\delta(t), T(t))$ approaches the point C at which the driving traction is equal to the critical value.

[1] It is assumed in Fig. 11 that $\theta_* < \theta_b < \bar{\theta}_*$.

8. Creep due to phase transformation

As described in Chapter 4, the experiment of Sammis and Dein[14] suggests that a solid may creep at constant load when it experiences a phase transformation. In this chapter, we discuss the possible occurrence of creep as predicted by our model, and we show that the predictions are in qualitative agreement with the experimental results reported in [14].

We consider loading by a soft device, with the load $\hat{T}(t)$ at t given by

$$\hat{T}(t) = \begin{cases} T\,t/t_1, & 0 \le t \le t_1; \\ T, & t > t_1, \end{cases} \tag{8.1}$$

corresponding to ramp loading until time t_1, followed by a constant load T. The outer wall temperature θ_b is kept constant in the range (θ_*, θ^*). The annular cylinder is said to creep if the displacement $\delta(t)$ at the inner wall varies with time in the time interval $[t_1, \infty)$ during which the load remains constant at the value T. After the constant-load stage is reached, the creep rate at the inner wall is found from (7.1) to be given by

$$\dot{\delta}(t) = \frac{\partial \hat{\delta}}{\partial s}(T; s(t), \theta_b)\,\dot{s}(t), \quad for\ t > t_1, \tag{8.2}$$

where the radius s(t) of the phase boundary at time t is the solution of the ordinary differential equation (6.6) that satisfies the initial condition

$$s(t_1) = s_1. \tag{8.3}$$

Here $s_1 \in (r_3^*, b]$ is the radius of the phase boundary at the end of the ramp loading period. One may have either $s_1 = b$ or $s_1 < b$. In the former case, the ultimate load level T is too small to have initiated a phase transformation during the ramp period. In the latter case, a phase transformation has been initiated during the ramp period, and the phase boundary has already moved inward to

$r = s_1$ by the time the ultimate load level T is reached. (See the discussion in the previous chapter concerning constant-rate loading processes.)

Since by (5.33) the temperature distribution $\theta(r,t)$ depends on the time only through the phase boundary radius s(t) when the outer wall temperature θ_b is kept constant, one may write $\theta(s(t),t) \equiv \theta(s(t),\theta_b)$, where we have also indicated explicitly in the notation the dependence on the outer wall temperature θ_b. By (6.2), we may then rewrite the kinetic relation (6.6) in the form

$$-\dot{s}(t) = V^*(s(t);T,\theta_b), \quad for\ t > t_1, \tag{8.4}$$

where

$$V^*(s;T,\theta_b) = \hat{V}(h(\frac{T}{2\pi s},\theta(s,\theta_b)),\theta(s,\theta_b)), \tag{8.5}$$

while $\hat{V}$ is defined by (6.1). We note that the differential equation (8.4) is autonomous.

According to (8.2), the creep rate $\dot{\delta}(t)$ is zero if the radius of the phase boundary s(t) is constant for $t > t_1$. This occurs if and only if the differential equation (8.4) has the solution

$$s(t) \equiv s_1, \quad for\ t \geq t_1. \tag{8.6}$$

This in turn happens if and only if

$$V^*(s_1;T,\theta_b) = 0. \tag{8.7}$$

Thus creep is <u>absent</u> if and only if the initial radius s_1 is a zero of the kinetic response function $V^*(\cdot;T,\theta_b)$. Whether or not (8.7) holds will depend not only on the ultimate load level T and the value of the outer wall temperature θ_b, but in general on the particular kinetic response function and on the detailed values of the other constitutive parameters of the model as well.

For the loading program (8.1), for a specific kinetic response function $\hat{V}$ of the type shown in Fig. 7, and for suitably chosen values of the various constitutive parameters, we have numerically solved the initial value problem (8.4), (8.3) and determined the creep rate according to (8.2) for four different values θ_1, θ_2, θ_3, θ_4 of the outer wall temperature, ordered by $\theta_1 < \theta_2 < \theta_3 < \theta_4$. The results are shown in Fig. 12 as plots of $\dot{\delta}$ vs. time t. The computation shows that no creep occurs at the two lower temperatures, but significant creep rates have appeared at the higher temperatures. The qualitative features of these results agree with the observations of Sammis and Dein [14], which are sketched schematically in Fig. 13.

Our numerical results in Fig. 12 seem to suggest that

$$\lim_{t\to\infty} \dot{\delta}(t) = 0. \tag{8.8}$$

To see this long-term feature of creep, we assume that creep occurs after the ramp loading period under consideration. Let the arc OQA in Fig. 14 represent the response curve corresponding to the ramp loading period $[0, t_1]$. The subsequent response must correspond to a horizontal line segment starting at the point A, say AB. By the property of the autonomous equation (8.4), the final radius s_f of the phase boundary corresponding to the point B must be such that

$$V^*(s;T,\theta_b)\begin{cases} > 0, & s > s_f; \\ = 0, & s = s_f. \end{cases} \tag{8.9}$$

This assures that the autonomous equation (8.4) can be integrated as

$$t = t_1 + \int_s^{s_1} \frac{dr}{V^*(r;T,\theta_b)}, \quad s > s_f. \tag{8.10}$$

The integral in (8.10) is divergent as s tends to s_f if

$$\lim_{s\to s_f} \frac{V^*(s;T,\theta_b)}{s - s_f} = 0. \tag{8.11}$$

Any kinetic response function V^* with the property (8.11) thus gives

$$\lim_{t\to\infty} s(t) = s_f, \quad \textit{and} \quad \lim_{t\to\infty} \dot{s}(t) = 0. \tag{8.12}$$

The long-time result (8.8) then follows from (8.2) and (8.12).

9. The shape-memory effect

For $\theta \in (\bar{\theta}_*, \bar{\theta}^*)$, the Helmholtz free energy potential $\Psi(\cdot, \theta)$ in (3.21) has two wells (see Fig. 15), with corresponding local minima at $\gamma = 0$ and at $\gamma = \gamma_0(\theta)$ and correspondingly, the stress-strain response curve has the form shown in the Fig. 3(c). This allows the body to achieve an unstressed but deformed state through a mechanical cycling process at the fixed temperature θ, starting at the undeformed state. The residual deformation can be removed through a temperature cycling process, because the unstressed state must also be undeformed as long as $\theta \in (0, \bar{\theta}_*) \cup (\bar{\theta}^*, \infty)$. Fig. 16 illustrates the so-called shape-memory behavior.

To see the shape-memory effect in the simple setting of finite anti-plane shear of the annular cylinder, we consider a mechanical cycling process T = T(t), θ_b = constant, followed by a thermal cycling process $\theta_b = \theta_b(t)$, T = constant:

$$T(t) = \begin{cases} T_0\, t, & 0 \le t < 1; \\ T_0\,(2-t), & 1 \le t < 2; \\ 0, & 2 \le t \le 3, \end{cases} \tag{9.1}$$

$$\theta_b = \theta_b(t) = \begin{cases} \theta_1, & 0 \le t < 2; \\ \theta_1 + \frac{5}{4}(\theta_1 - \bar{\theta}_*)(2-t), & 2 \le t < 2.8; \\ \theta_1 - 5(\theta_1 - \bar{\theta}_*)(3-t), & 2.8 \le t \le 3, \end{cases} \tag{9.2}$$

where $\theta_1 \in (\bar{\theta}_*, \bar{\theta}^*)$ and $T_0 \ge T_*(\theta_1)$.

The macroscopic response arising from this program of thermo-mechanical loading is shown schematically in Fig. 17. During the mechanical cycling period, the $T - \delta$ response is represented by the path OQPZD, and some residual deformation is clearly produced (see Section 7.2 for details). The mechanical load T vanishes identically during the temperature cycling period; the thermal response δ vs. θ_b is shown in Fig. 17(b). After the wall temperature θ_b begins to drop, the

phase boundary moves towards the outer wall, and the point $(\delta(t), \theta_b(t))$ moves along the curve DE. At the point E, the phase boundary disappeared at the outer wall and the residual deformation is removed. The point $(\delta(t), \theta_b(t))$ moves along the line segment EF as θ_b continues decreasing to $\bar{\theta}_*$, and it moves along the line segment FO when θ_b increases from $\bar{\theta}_*$ to θ_1. Neither phase transformation nor deformation accompanies this stage of the process.

We have made a numerical simulation to demonstrate the shape-memory behavior of the annular cylinder during the thermo-mechanical loading process described by (9.1) and (9.2). For appropriately chosen values of the constitutive parameters, Fig. 18 shows the configurations of half a cross section of the body at a sequence of time instants.

During the mechanical cycling process, a phase transformation is initiated and a 1,3-phase boundary emerges at the outer wall of the cylinder when the mechanical load reaches a certain level. The phase boundary moves towards the inner wall until it coincides with the surface $\mathrm{r} = r_3^*(\theta_1)$ as the load continues to increase. This is shown by Fig. 18(a) and (b) in which the darker area represents the part of the body where the material is in phase-3. As we have discussed in Chapter 7, the phase boundary remains at $\mathrm{r} = r_3^*(\theta_1)$ when the load T(t) continues to increase (see Fig. 18(b) and (c)). From Fig. 18(c), (d) and (e), one can see that the load T(t) decreases from its maximum T_0, the phase boundary stays at $\mathrm{r} = r_3^*(\theta_1)$, and it moves backwards only after the load drops below a certain level. Fig. 18(f) shows that at the end of mechanical cycling process, the body is in a two-phase equilibrium state and some residual deformation has been produced. During the temperature cycling process, the phase boundary continues to move towards the outer wall and disappears there as the outer wall temperature decreases. This is shown by Fig. 18(f), (g) and (h). Finally, Fig. 18(h) and (i) show that the body remains at the undeformed-unstressed state during the stage of temperature increasing. Therefore, we see that the residual

deformation produced by the mechanical cycling process has been removed during the temperature cycling process and the body has achived its original shape.

Appendix: A note on the constitutive parameters

As mentioned in Chapters 8 and 9, we have done some numerical work to exhibit the creep feature and the shape-memory behavior predicted by our model. It should be mentioned that the available experimental data is insufficient to permit the determination of all constitutive parameters needed in the model constructed here. For the purpose of making qualitative comparison with experiments we have made rather arbitrary choices of these parameters. For those readers who may be interested, we give here some details regarding our computation.

We have assumed that the heat conductives k_1 and k_3 are two different constants, and we have approximated the kinetic response function $\hat{V}$ by a piecewise linear function:

$$\hat{V}(f,\theta) = \begin{cases} s_M(f - d_M f_m(\theta)), & \mathrm{d}_M f_M < f < f_M; \\ 0, & \mathrm{d}_m f_m(\theta) \le f \le d_M f(\theta); \\ s_m(f - d_m f_m(\theta)), & \mathrm{f}_m(\theta) < f < d_m f_m(\theta), \end{cases} \quad \forall \theta \in [\theta_*, \theta^*].$$

where s_M, s_m, d_M and d_m are all constants.

The numbers we assigned to the constitutive parameters are listed in the following table; the first row was used for modeling creep and the second was used for modeling shape-memory behavior.

k_3/k_1	α	β_0/α	n	m	s_m	s_M	d_m	d_M
1.5	.04	1.35	3	9.5	.001	.01	2×10^6	4×10^2
1.5	.04	1.23	3	2.3	.001	.3	2×10^6	3×10^6

One may notice that the values of s_M and d_M in the first row are much smaller than those in the second row; this results in the fact that the phase boundary propagates comparatively more slowly, so that we have a better view in the plots of creep rate vs. time shown in Fig. 12.

REFERENCES

[1] L. Delaey, R.V. Krishnan, H. Tas and H. Warlimont, Review: Thermoelasticity, pseudo-elasticity and the memory effects associated with martensitic transformations, *Journal of Material Science*, 9(1974), 1521-1555

[2] J.K. Knowles, On the dissipation associated with equilibrium shocks in finite elasticity, *Journal of Elasticity*, 9(1979), 131-158

[3] R. Abeyaratne, Discontinuous deformation gradients in plane finite elastostatics of incompressible materials, *Journal of Elasticity*, 10(1980), 255-293

[4] R.D. James, Finite deformation by mechanical twinning, *Archive for Rational Mechanics and Analysis*, 77(1981), 143-176

[5] R.D. James, Displacive phase transformations in solids, *Journal of the Mechanics and Physics of Solids*, 34(1986), 359-394

[6] R. Abeyaratne and J.K. Knowles, Non-elliptic elastic materials and the modeling of dissipative mechanical behavior: an example, *Journal of Elasticity*, 18(1987), 227-278

[7] R. Abeyaratne and J.K. Knowles, Non-elliptic elastic materials and the modeling of elastic-plastic behavior in finite deformation, *Journal of the Mechanics and Physics of Solids*, 35(1987), 343-365

[8] P. Rosakis, Ellipticity and deformations with discontinuous gradients in finite elastostatics, to appear in *Archive for Rational Mechanics and Analysis*

[9] S. Silling, Phase changes induced by deformation in isothermal elastic crystals, Brown University Technical Report, NSF Grant MSM 8658107/2, February, 1988

[10] M.E. Gurtin, Two-phase deformations of elastic solids, *Archive for Rational Mechanics and Analysis*, 84(1983), 1-29

[11] J.D. Eshelby, The continuum theory of lattice defects, *Solid State Physics* (Edited by F. Seitz and D. Turnbull), Vol.3. Academic Press, New York

[12] R. Abeyaratne and J.K. Knowles, On the driving traction acting on a surface of strain discontinuity in a continuum, to appear in *Journal of the Mechanics and Physics of Solids*

[13] R. Abeyaratne and J.K. Knowles, On the dissipative response due to discontinuous strains in bars of unstable elastic material, *International Journal of Solids and Structures*, 24(1988), 1021-1044

[14] C.G. Sammis and J.L. Dein, On the possibility of transformational superplasticity in the earth's mantle, *Journal of Geophysical Research*, 79(1974), 2961-2965

[15] J.K. Knowles, On finite anti-plane shear for incompressible elastic materials, *Journal of the Australian Mathematical Society*, Series B, 19(1976), 400-415

[16] J.K. Knowles, The finite anti-plane shear field near the tip of a crack for a class of incompressible elastic solids, *International Journal of Fracture*, 13(1977), 611-639

[17] J.K. Knowles and A.J. Rosakis, On the scale of the nonlinear effect in a crack problem, *Journal of Applied Mechanics*, 108(1986), 545-549

[18] Q. Jiang and J.K. Knowles, A class of compressible elastic materials capable of sustaining finite anti-plane shear, to appear in *Journal of Elasticity*

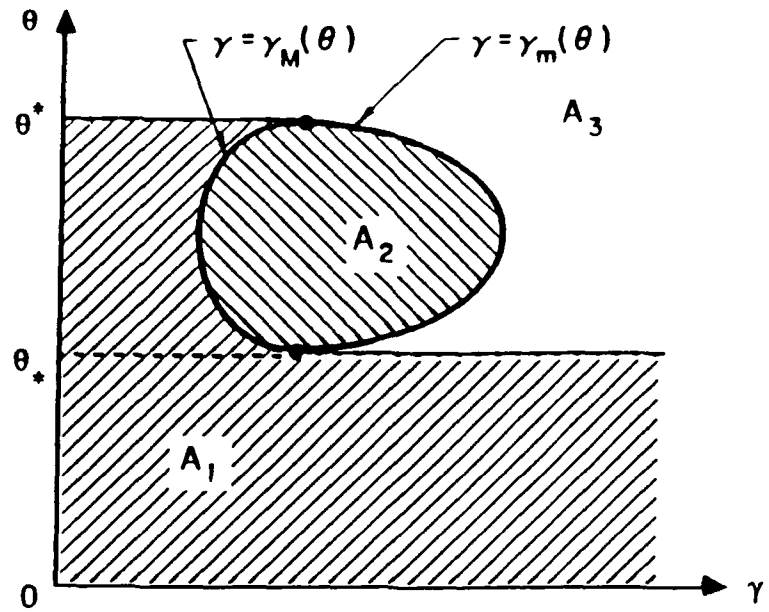

Fig. 1. The sets of points in the strain-temperature plane

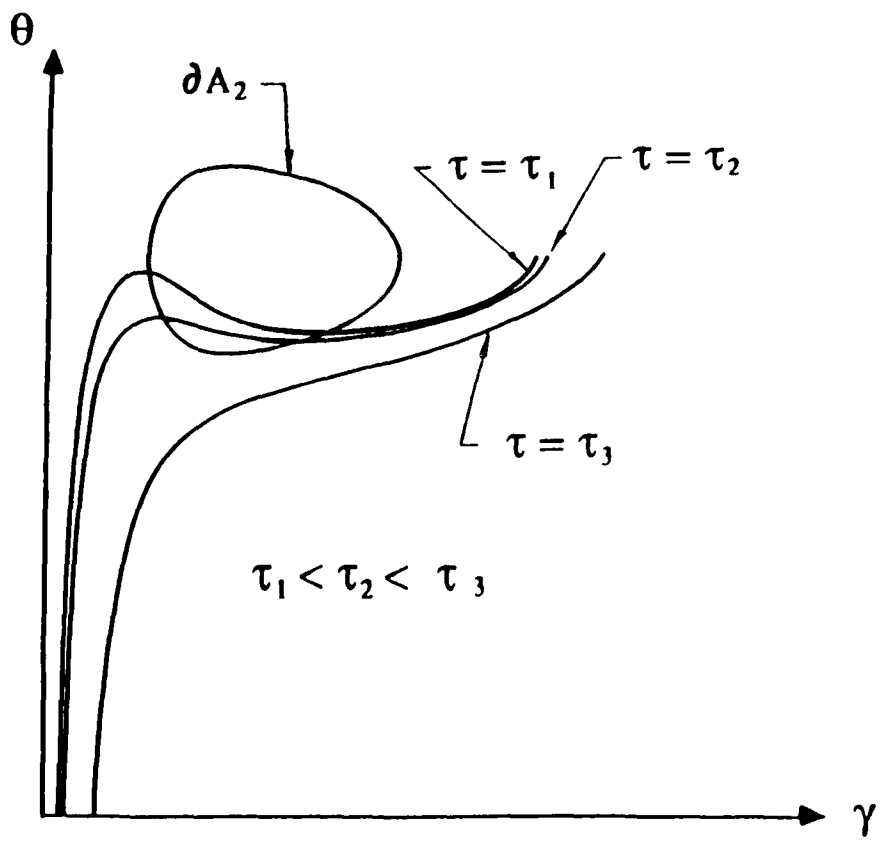

Fig. 2. Constant-stress curves

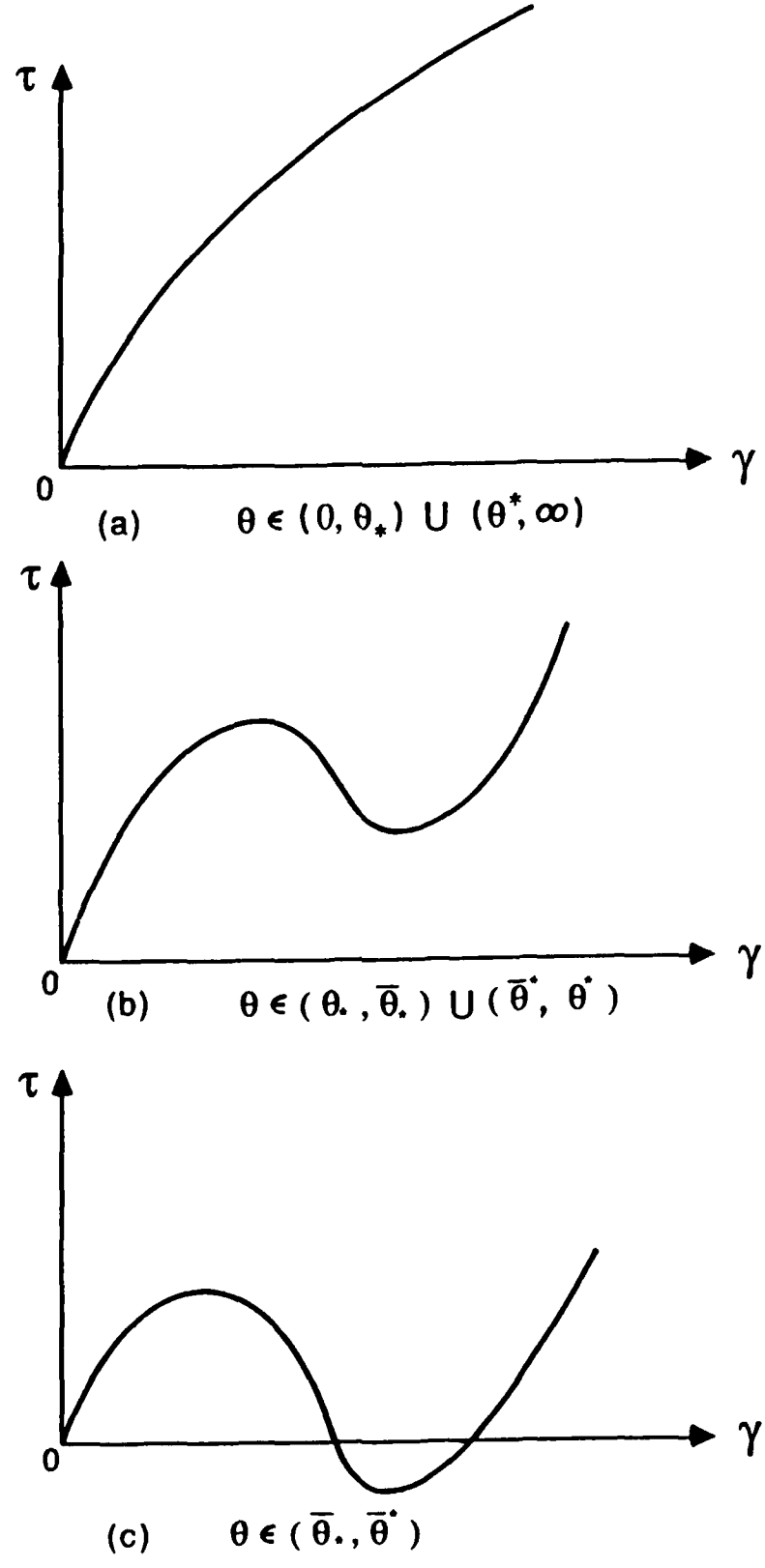

Fig. 3. Stress strain response curves

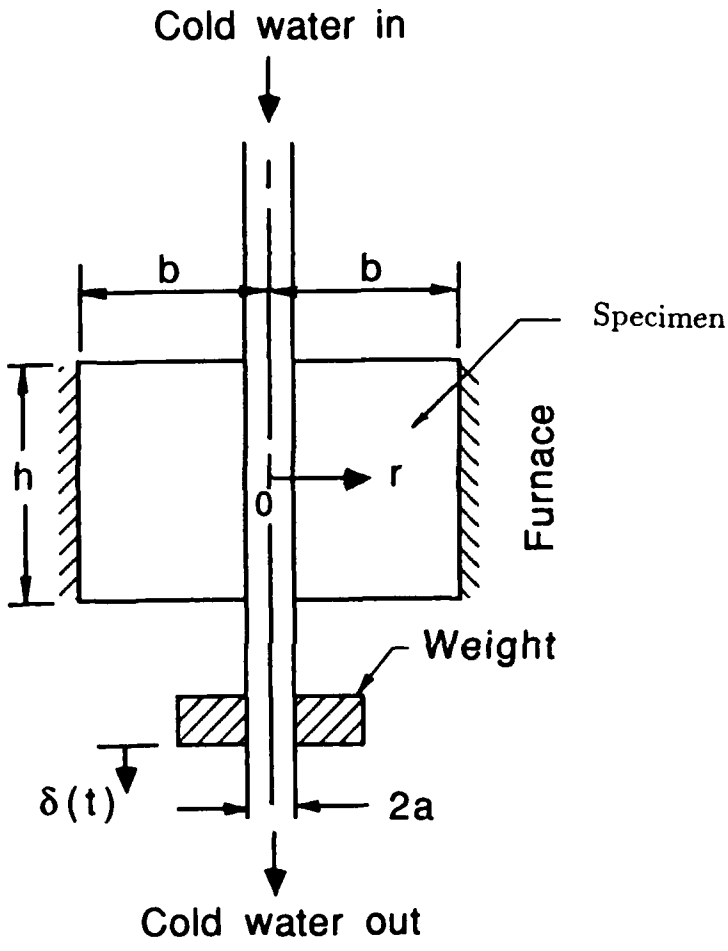

Fig. 4. Sammis and Dein's experiment

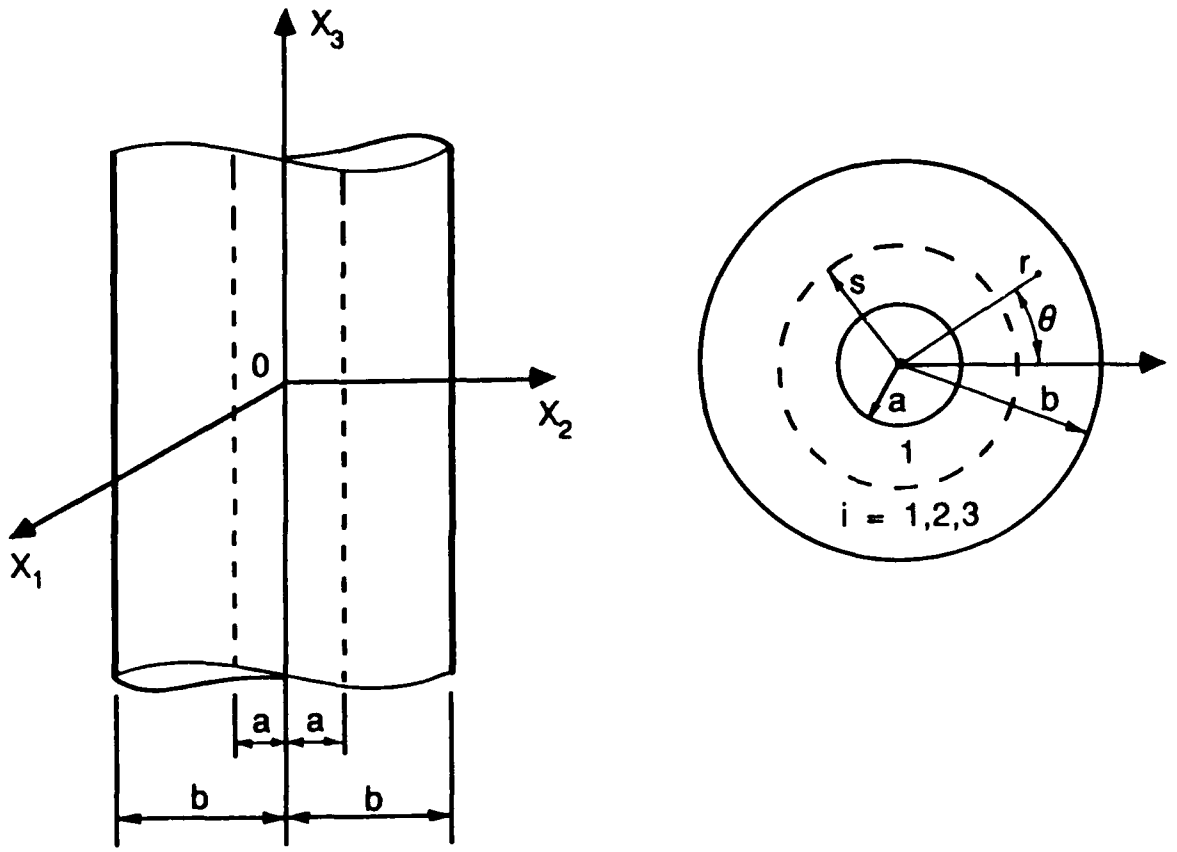

Fig. 5. The annular cylinder

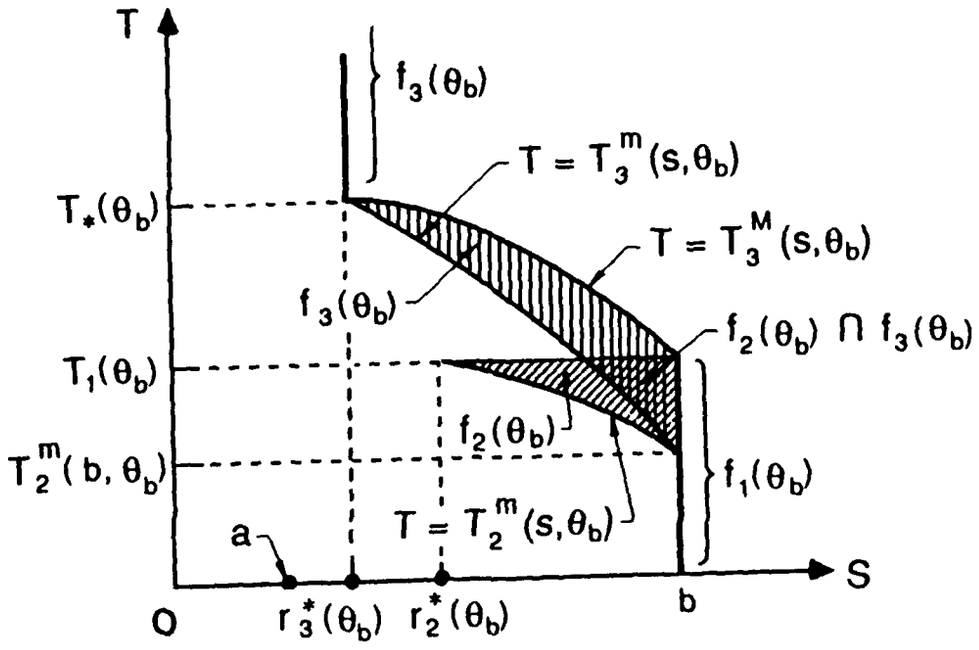

(a) $\theta_* < \theta_b \leqslant \overline{\theta}_*$

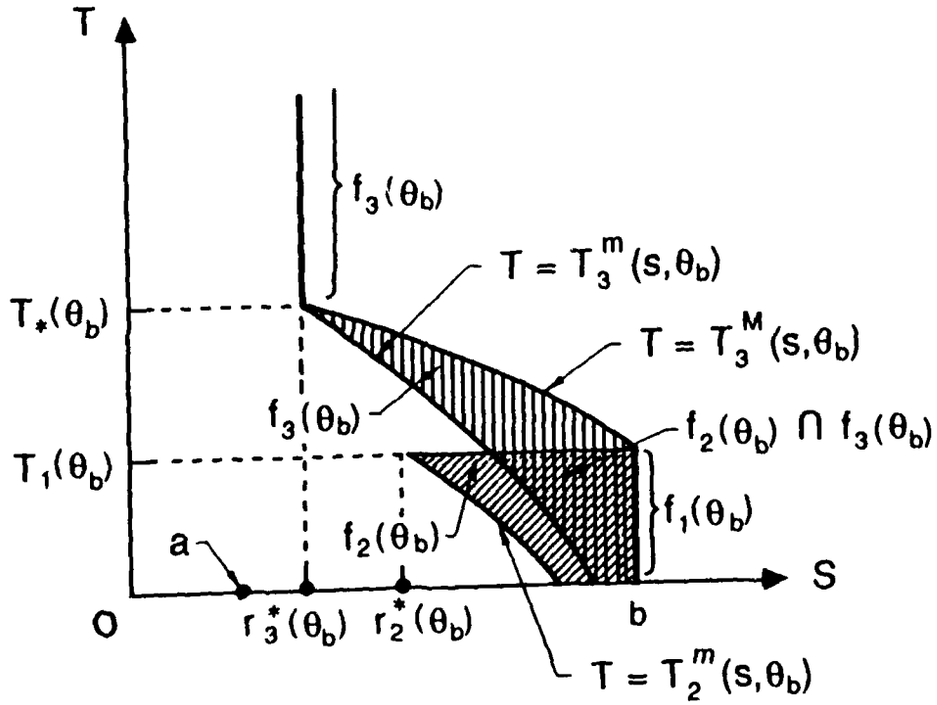

(b) $\overline{\theta}_* < \theta_b < \overline{\theta}_*$

Fig. 6. Parameter sets $f_1(\theta_b)$, $f_2(\theta_b)$, $f_3(\theta_b)$ in s,T-plane

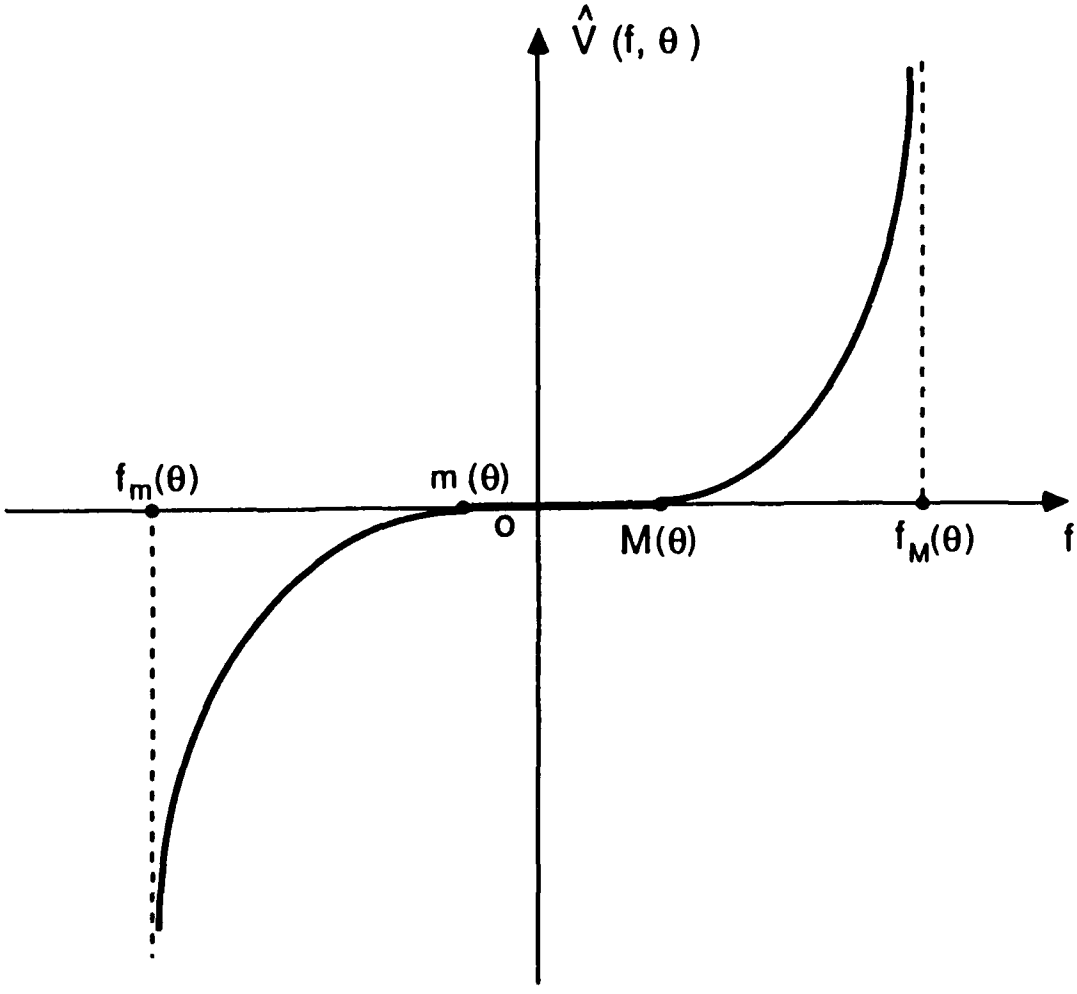

Fig. 7. Kinetic response function

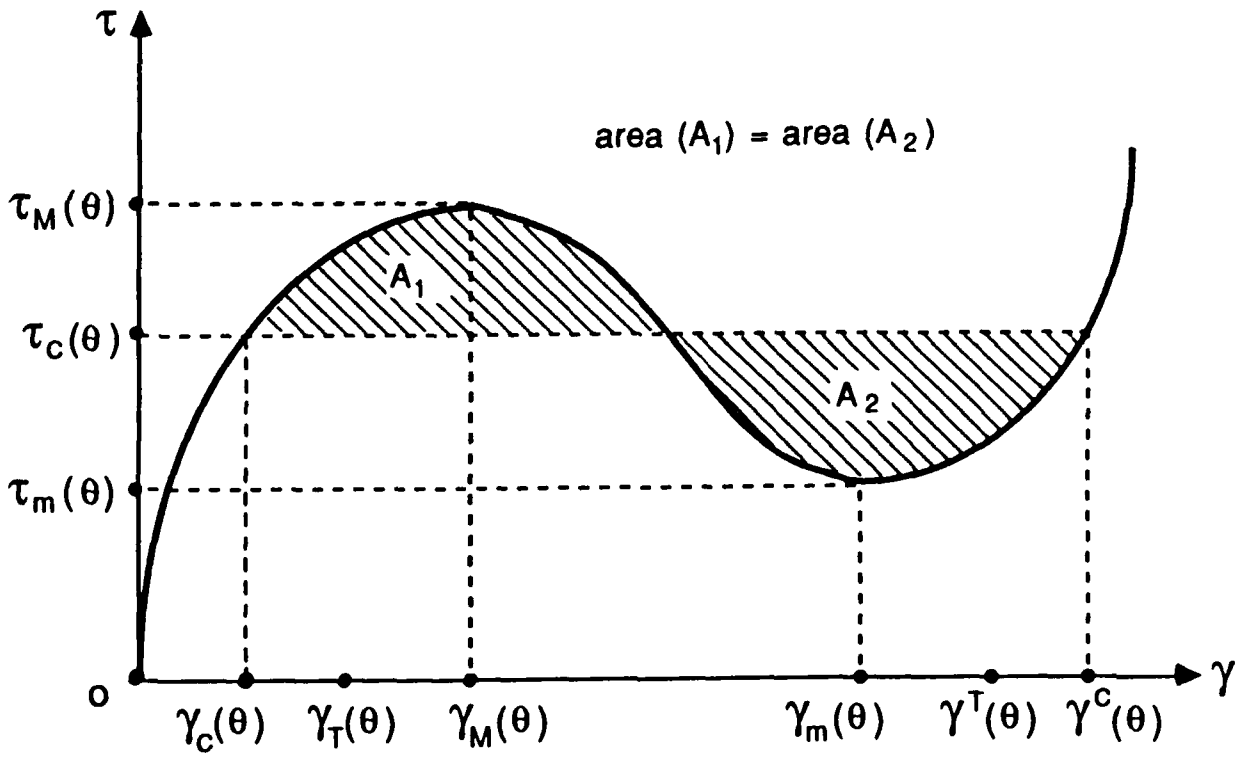

Fig. 8. The transformation strains $\gamma_T(\theta)$, $\gamma^T(\theta)$

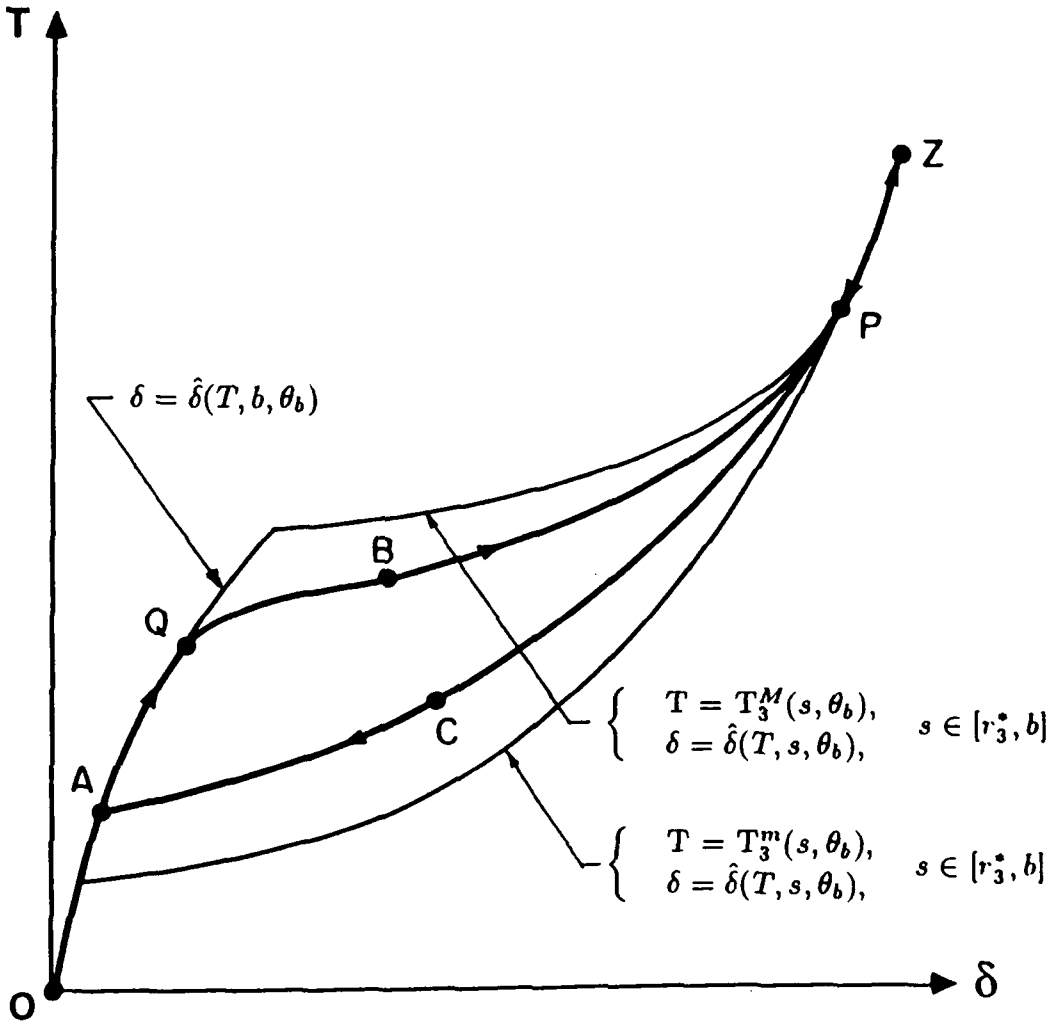

Fig. 9. Loading-unloading path

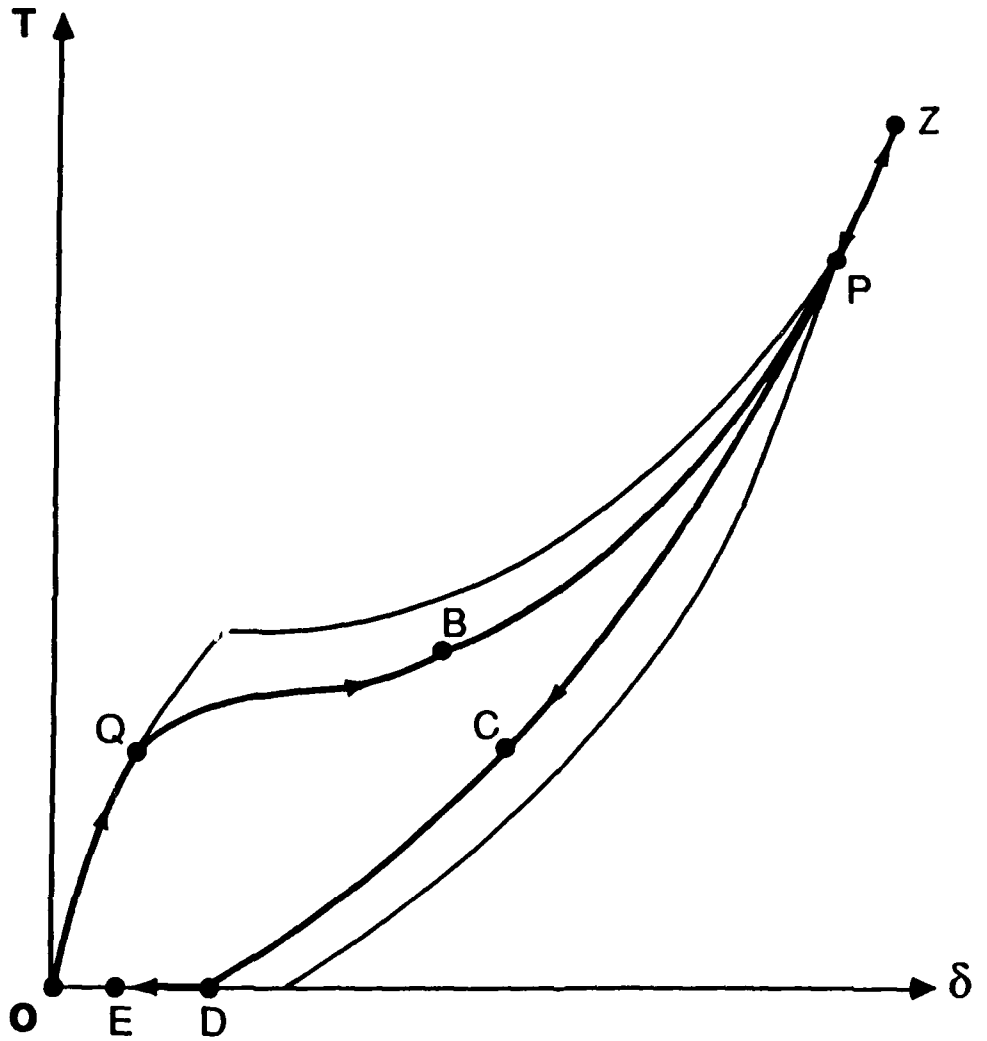

Fig. 10. Residual deformation

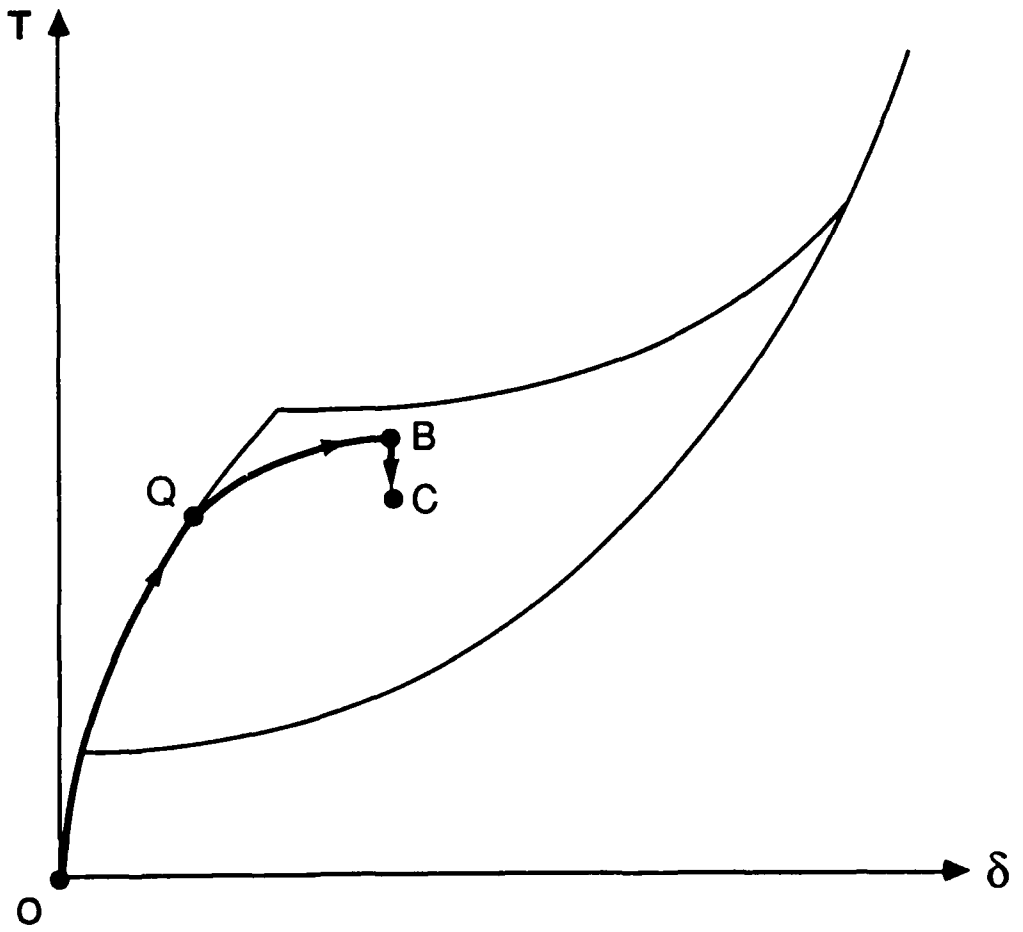

Fig. 11. Load relaxation

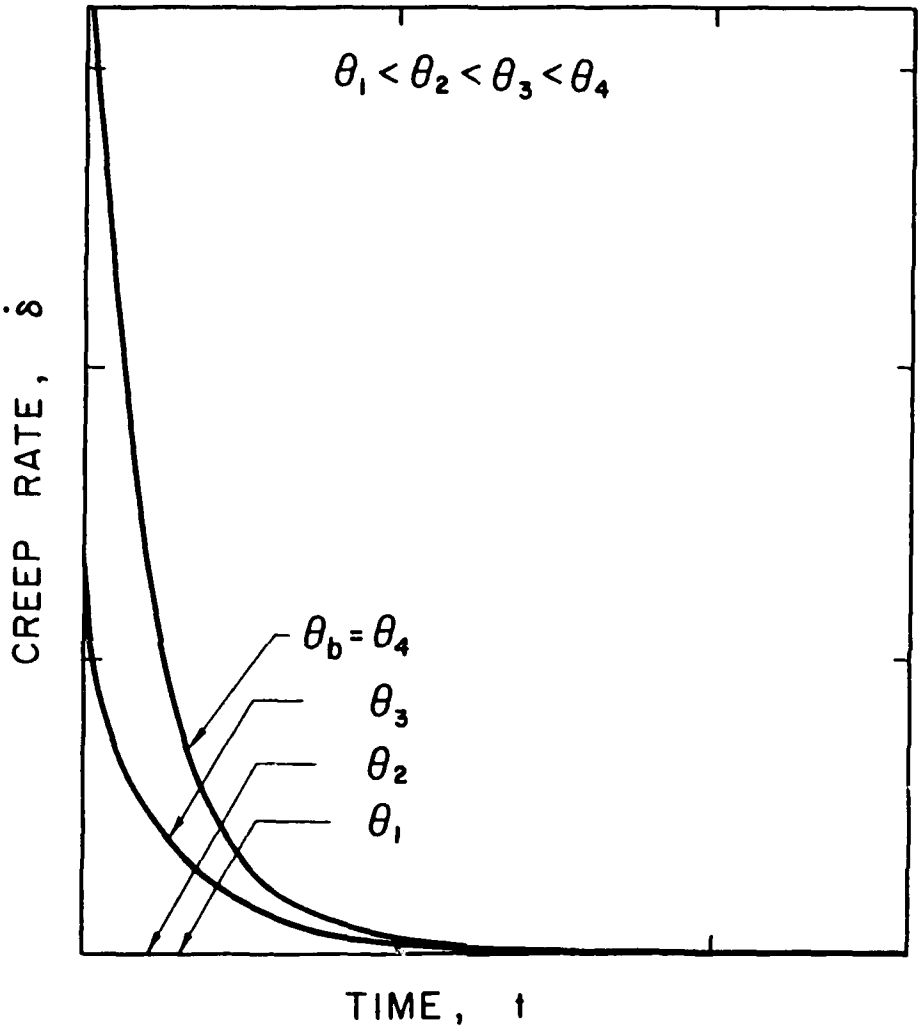

Fig. 12. Plots of creep rate $\dot{\delta}$ vs. time t as predicted by the present model

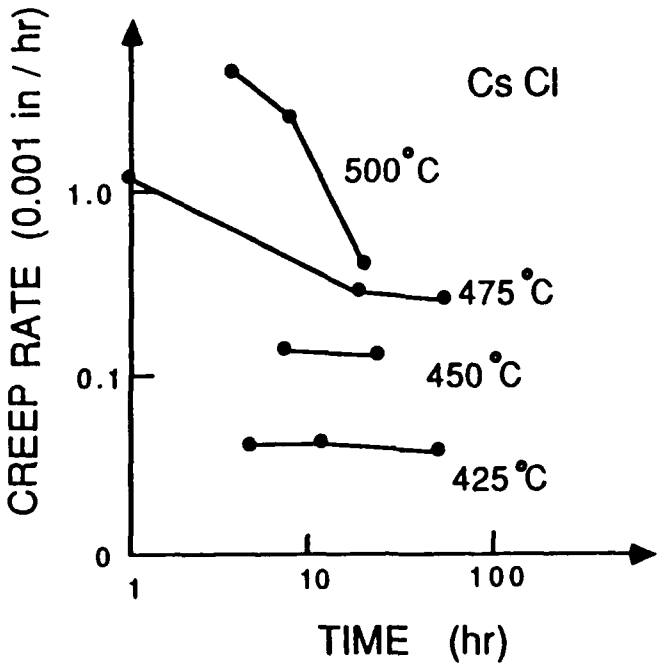

Fig. 13. Sammis and Dein's experimental data (note logarithmic scales)

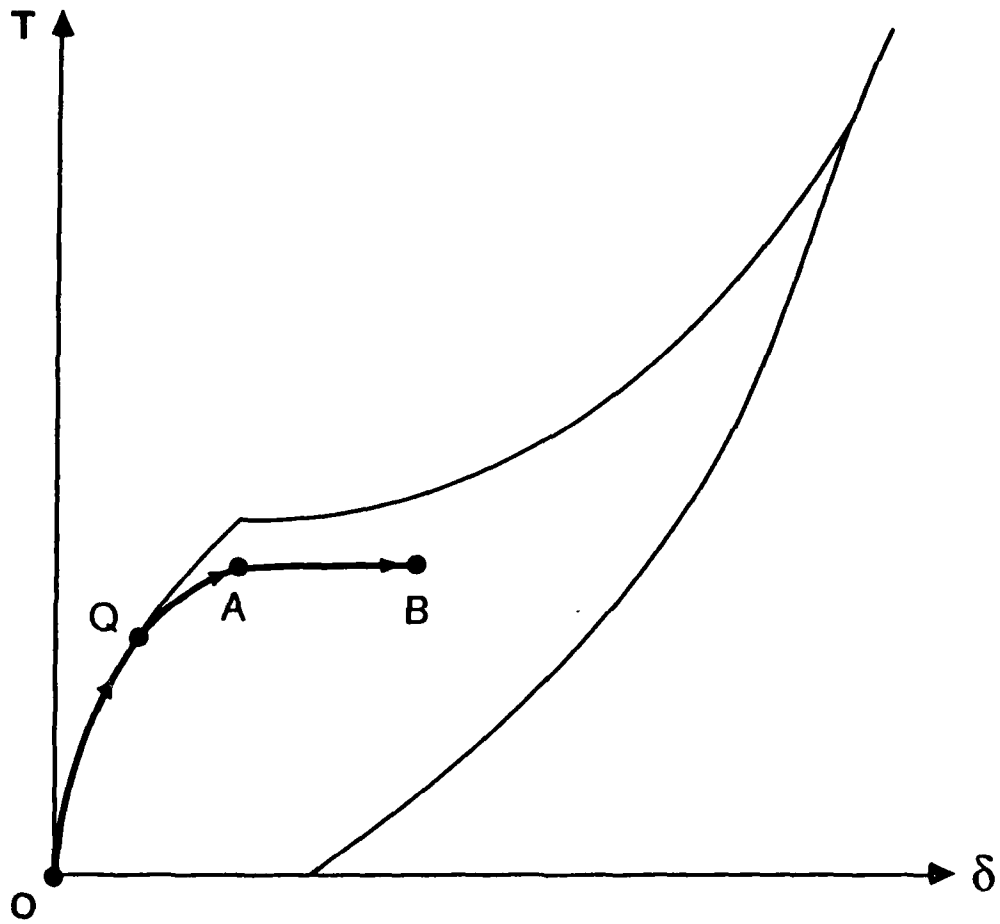

Fig. 14. Creep response curve in the δ,T-plane

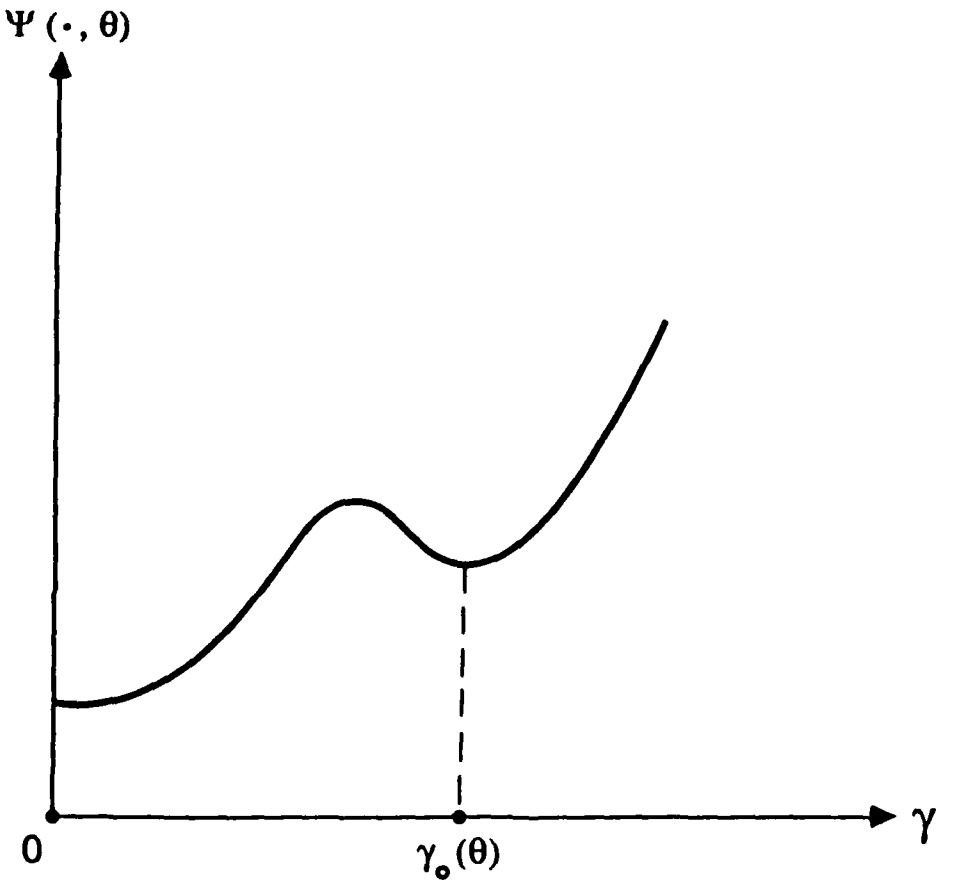

Fig. 15. Helmholtz free energy potential when $\theta \in (\bar{\theta}_*, \bar{\theta}^*)$

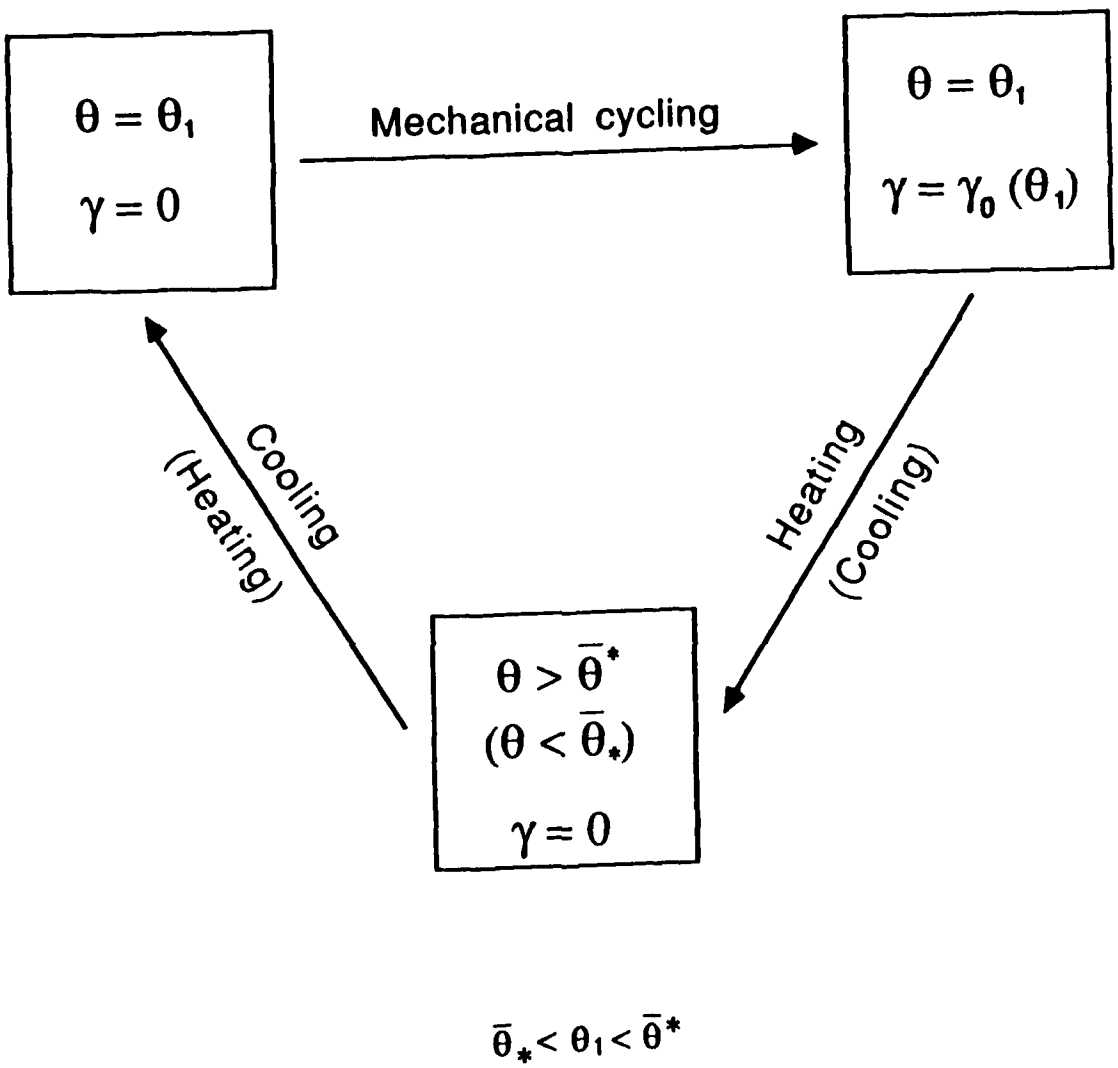

Fig. 16. Illustration of shape-memory behavior

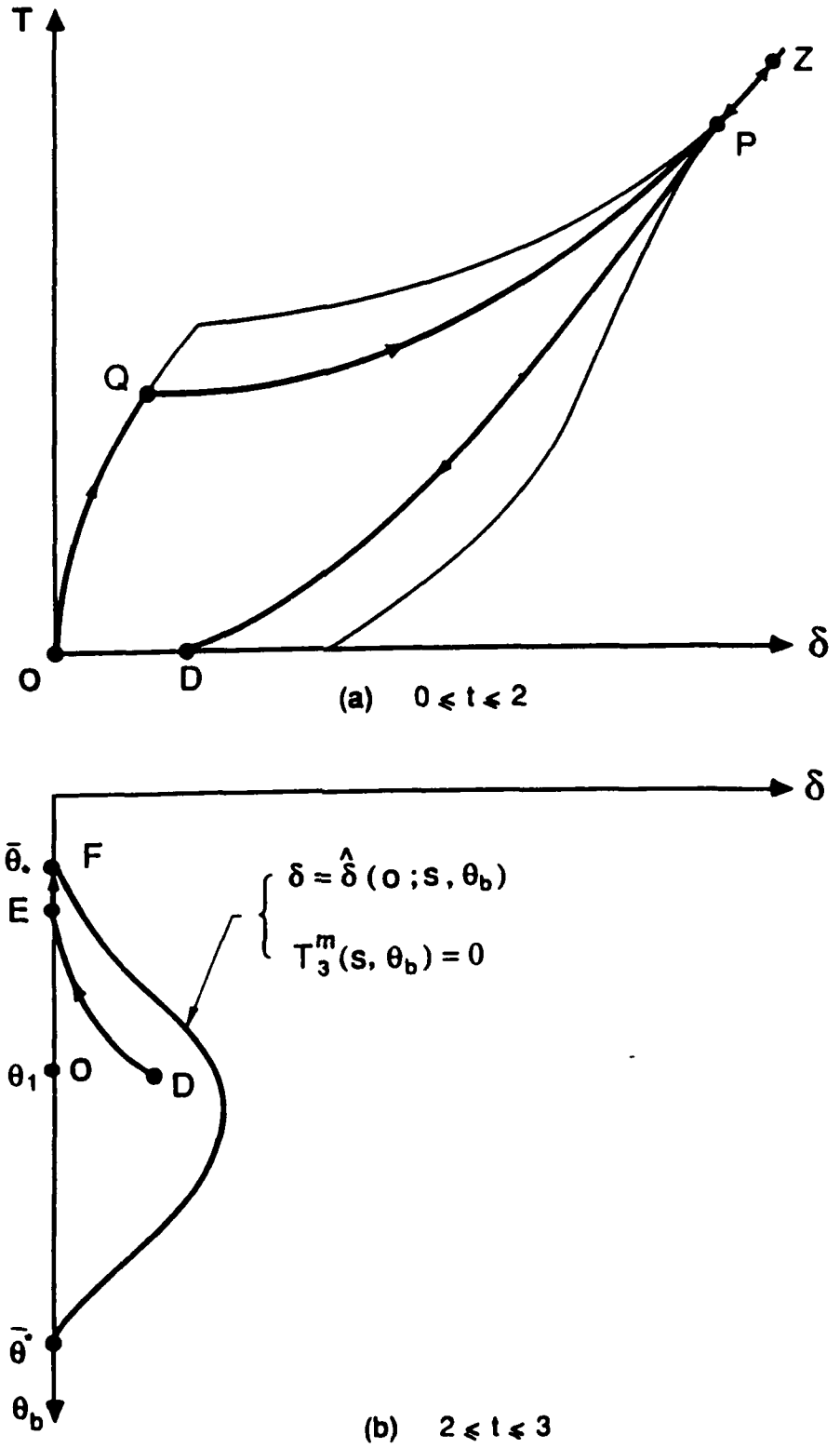

Fig. 17. Macroscopic response of the cylinder during a process illustrating shape-memory effect

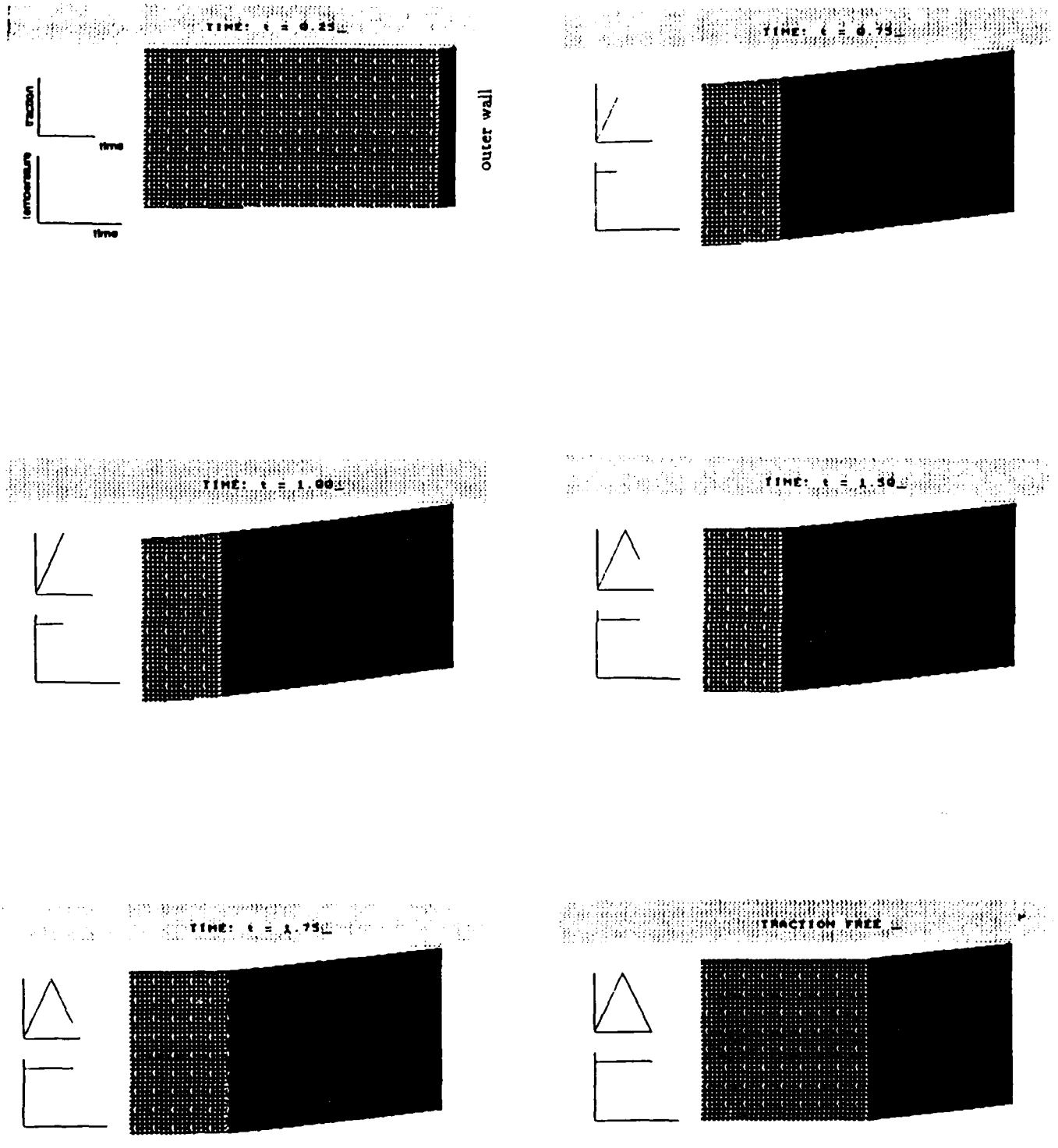

Fig. 18. Selected frames from simulation of shape-memory effect

(continued on next page)

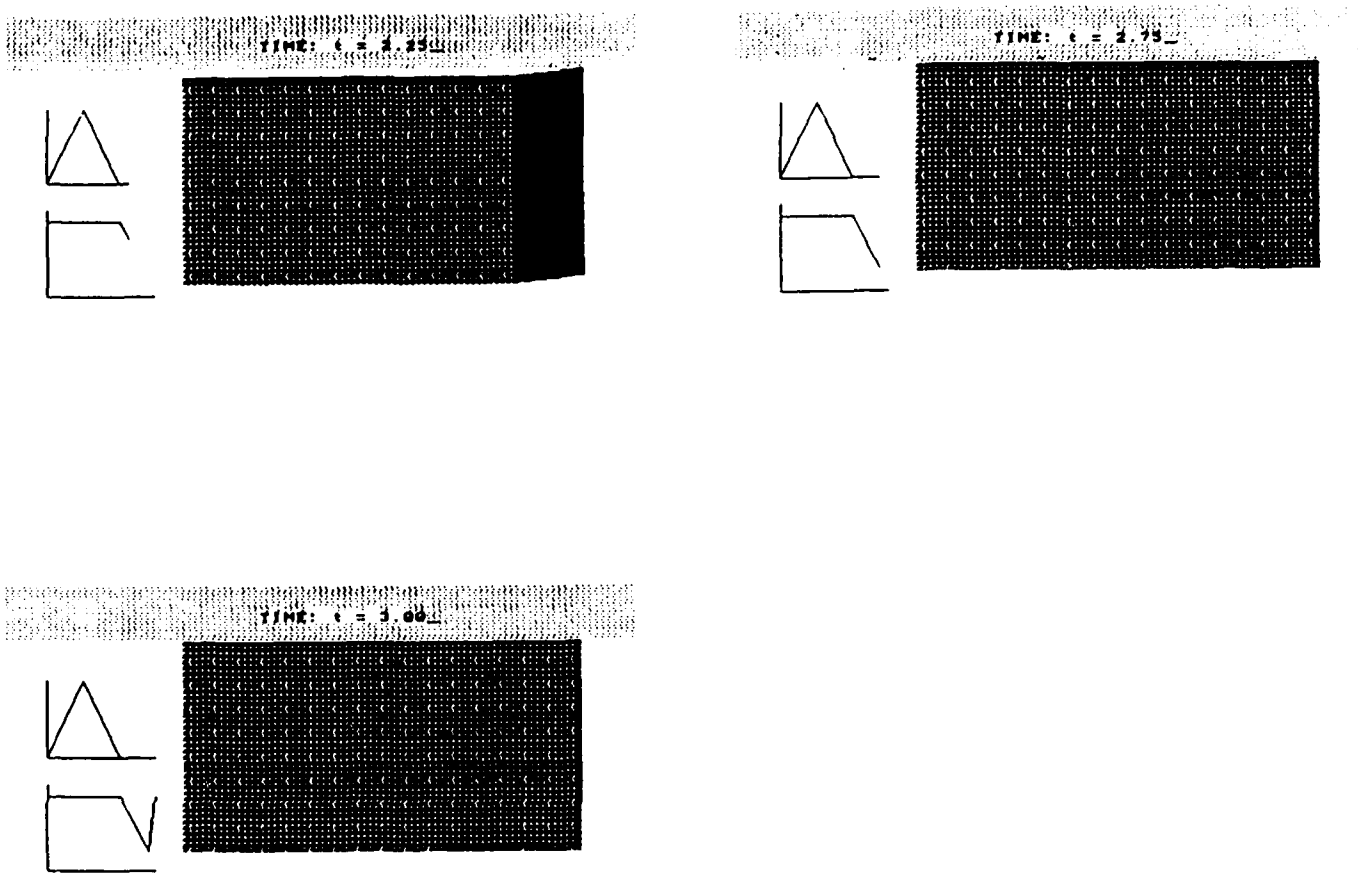

Fig. 18. Selected frames from simulation of shape-memory effect

(continued from preceding page)